10-11-1982

Effects on Electrolytic Cells of Magnetic Fields Applied to Single Electrodes

Craig Allen Cousins
Portland State University

AN ABSTRACT OF THE THESIS OF Craig Allen Cousins for the Master of Science in Physics presented October 11, 1982.

Title: Effects on Electrolytic Cells of Magnetic Fields Applied to Single Electrodes.

APPROVED BY MEMBERS OF THE THESIS COMMITTEE:

[redacted]

John Dash, Chairperson

[redacted]

M. Takeo

[redacted]

Gary L. Gard

[redacted]

Gertrude F. Rempfer

The primary goal of this research was to investigate the effects associated with the application of magnetic fields to single electrodes.

There were two basic systems studied. The first system was the electrolysis of water containing H_2SO_4 and the second system was the electrolytic transportation of copper from the anode to the cathode utilizing an electrolyte of 0.5 M H_2SO_4 and 0.5 M $CuSO_4$ in a solvent of deionized H_2O.

For the first system, the most notable effects were: (a) a

decrease in the amount of gas collected above the exposed electrode, (b) heating in the direction of the Lorentz force or, what was more commonly observed, cooling in the opposite direction in that portion of the cell located between the two electrodes and (c) variations in the temperatures observed approximately 1 cm above the electrodes following the application or removal of an applied magnetic field to a single electrode.

For this first system the observed changes in cell voltage were so small that even when the constant current mode was utilized long term "noise" in the system effectively overshadowed any measurement of the effect of applied magnetic fields on the cell voltage for extended time periods.

Since previous authors had studied the effect of applied magnetic fields on the electrolysis of copper and observed fairly large changes in the total cathode polarization being noted, this system appeared to be a reasonable candidate for further studies. The primary effects investigated using this system were the effects of pumping, of applied magnetic fields and of a combination of the two on the cell voltage.

Pumping the electrolyte into the top of the center tube and out the top of the other two tubes was also attempted with the first system; however, bubbles produced during the electrolytic process clouded the cell voltage readings so completely that it was impossible to assess what effect the combination of pumping and applied magnetic field had on the cell voltage.

Using the electrolysis of copper system and comparing the

results obtained for the anode, cathode and the combination of anode and cathode between the pole pieces, it was noted that the largest voltage drop observed following the application of the magnetic field was for the single cathode. This voltage drop was approximately 1.5 times that recorded for the anode-cathode combination and several times the value observed for the single anode.

These results are interpreted as showing that a decrease in the cell voltage is to be expected when either the anode or the cathode is exposed to an applied $\vec{B}$ field. The decrease in the cell voltage is apparently due to a reduction in the apparent thickness of the diffusion layer. This idea is substantiated by the complementary nature of the voltage drop observed following the application of the $\vec{B}$ field and the quantitatively similar effect associated with pumping. The fact that the voltage drop associated with the anode-cathode combination is less than that observed for the single cathode is apparently due to magnetoresistance.

Most of the data presented in this thesis, with the notable exception of the observed gas volumes, was processed and recorded by an AIM 65 microcomputer which was interfaced with the various sensing equipment through a Fluke Digital Multimeter (Model 8800 A). The magnetic field was applied with a water-cooled electromagnet, except for one case in which a permanent magnet was used.

EFFECTS ON ELECTROLYTIC CELLS OF MAGNETIC FIELDS APPLIED TO SINGLE ELECTRODES

by

CRAIG ALLEN COUSINS

A thesis submitted in partial fulfillment of the requirements for the degree of

MASTER OF SCIENCE
in
PHYSICS

Portland State University

1982

TO THE OFFICE OF GRADUATE STUDIES AND RESEARCH:

The members of the Committee approve the thesis of Craig Allen Cousins presented October 11, 1982.

[redacted]

John Dash, Chairperson

[redacted]

M. Takeo

[redacted]

Gary L. Gard

[redacted]

Gertrude F. Rempfer

APPROVED:

[redacted]

R. W. Sommerfeldt, Head, Department of Physics

[redacted]

Stanley E. Rauch, Dean of Graduate Studies and Research

ACKNOWLEDGEMENT

I wish to thank Drs. John Dash, M. Takeo and Gertrude Rempfer for their suggestions and discussions which added greatly to this thesis. In addition, I am indebted to Mrs. Lisa Yamamoto for typing this thesis and to Mrs. Marie Brown for her general guidance in the preparation of this thesis.

This research was sponsored by U.S. Army Research Office.

TABLE OF CONTENTS

LIST OF TABLES

LIST OF FIGURES

FIGURE PAGE

FIGURE PAGE

CHAPTER I

INTRODUCTION

Experiments to determine the effect of magnetic fields on the electrodeposition of chromium often gave inconclusive results due to the complexities of the chromium plating process. For example, some of the hydrogen gas produced in this process is trapped in the chromium plating. This, in combination with other factors, makes it difficult to quantify the effect of a magnetic field on hydrogen gas production. A less complex system, the electrolysis of water, was therefore chosen for these studies.

In order to investigate the effects (on the electrolytic process) of an applied $\vec{B}$ field, in conjunction with pumping the electrolyte through the cell, an electrolytic solution for plating copper was used. Complications due to gas evolution are thus avoided.

The primary effects discussed in this paper are those related to changes in cell voltage, temperature and effects on gas production and collection.

BACKGROUND MATERIAL

In this section, a brief theoretical discussion of the polarization process associated with electrolytic reactions is presented (1). This is followed by a short discussion of some of the effects associated with applied magnetic ($\vec{B}$) fields on electrolytic systems.

Polarization

The total polarization (i.e. the difference between the observed and rest or equilibrium potentials) is made up of several distinct parts: included among these are (1) ohmic, (2) activation and (3) concentration effects. Polarization due to ohmic effects shows up immediately following the application of the cell current, while activation effects require time on the order of milliseconds. Finally, polarization effects due to concentration build up more slowly with time. When the current is turned off, polarizations due to these three factors disappear in the same order.

Examining the three basic types of polarization, as a function of current, it is observed that ohmic polarizations are linear, while concentration polarizations increase exponentially; finally, for activation polarization a rapid rise followed by a more gentle increase is observed.

An important concept, which should be mentioned, is the double layer. In order to understand this phenomenon let us examine first of all the case in which there is no external current flow.

When a metal electrode is immersed in an electrolytic solution, a few of the metallic atoms lose electrons and enter the solution as ions. These cations and others are attracted by the excess negative charges associated with the metal electrode, thus forming a Helmholtz or double layer composed of a "layer" of free electrons in the metal and a neighboring layer of cations in the electrolyte. Associated with this double layer is some definite potential difference.

As one travels away from the electrode, beyond the double layer,

one encounters a diffuse layer in which the anions outnumber the cations. This is due to the fact that anions are attracted to the cations which make up the outer portion of the double layer. For dilute solutions, this diffuse layer may be up to 10 atomic diameters in thickness. However, for more concentrated solutions, the diffuse layer is much thinner.

Turning our attention once again to the double layer, it should be noted that this functions as an electrical condenser. Whenever the potential is changed, there is an accompanying change in the ionic concentration at the interface. That is, if the electrode is made more negative, ions will be drawn across the interface to the electrode and deposited. Similarly if the electrode is made more positive more ions will be given off by the metal and the metal will gradually dissolve. The only potential at which dissolution and deposition proceed at the same rate for a given electrode is the rest potential.

Concentration Polarization. At the surface of a working electrode, changes in concentration set up a concentration gradient between the solution at the electrode and that found in the bulk of the solution. When a steady current is employed, a steady state situation may be reached in which diffusion counterbalances depletion or accumulation. The rate of diffusion is determined primarily by the magnitude of the concentration gradient.

Suppose we approximate the diffusion rate as being linear with respect to concentration gradient. Then, according to Fick's law, the rate of diffusion, R_1, is given as:

$$(1\text{-}1) \qquad R_1 = \frac{A\,D}{\delta}(a - a_s).$$

In equation (1-1), A is the electrode area, D is the diffusion coefficent, δ is the apparent thickness of the diffusion layer (based on the assumption that the concentration gradient is approximately linear and may be approximated as being of thickness δ), a_s is the activity of the electrolyte at the electrode surface and a is the corresponding activity in the bulk solution.

For an unstirred solution near room temperature, a common value of δ is approximately 0.05 cm (1). If the solution is stirred, δ may be as thin as 0.001 cm.

Activation Polarization. The observed effect of temperature on reaction rates, is much greater than one would expect. For example, near room temperature, if the temperature is increased by 10°C, the reaction rate is doubled or even tripled while the average thermal energy is only increased by about 3.3%.

The above seems to imply that only a relatively small number of molecules, with energies much greater than the average, are actually taking part in the reaction (in agreement with the Boltzmann energy distribution).

The excess energy, which is required for the reaction, is termed the activation energy and may be supplied either thermally, by the electrode potential, or by a combination of the two.

Under equilibrium conditions, deposition and dissolution are taking place at the same rate. When cathodic conditions are imposed, the potential is made more negative. This increases the deposition rate while decreasing the dissolution rate. Therefore, deposition

predominates. Similarly under anodic polarization conditions solution predominates.

Effects of Applied Magnetic Fields on Electrolytic Processes

There are many observable effects of $\vec{B}$ fields on electrolytic processes. For this reason, there has been a great deal of theoretical and experimental work devoted to this area. In this thesis, the only effects discussed are those observed in conjunction with the cell temperature, cell voltage and gas collection.

The first effect to be discussed is magnetoresistance. Some experimental measurements of magnetoresistance were obtained by D. Laforgue-Kantzer (2). These measurements were accomplished by placing a small cell completely between the pole pieces of an electromagnet. Then, an alternating current of 1000 cps was applied. (The alternating current was used to avoid concentration polarization.) From this experiment, the change in resistance as a function of the applied $\vec{B}$ field was determined. The following quote is the result of that experiment:

> It (the magnetoresistance) is reasonably symmetrical for values of opposite induction. It is almost zero between -0.30 and +0.30 tesla and it rises up to 15% (of the normal resistance) at ±0.80 tesla.

For the experiment described above, the applied electric field was at right angles to $\vec{B}$ and very little data was given concerning the electrolyte.

One point, which should be emphasized, is that the magnetoresistance falls off rapidly with decreasing $\vec{B}$. Noting, in conjunction with this, that the magnitude of $\vec{B}$ decreases rapidly as one moves away

from the region enclosed by the pole pieces, it seems reasonable to assume that the primary area affected would be limited to that portion of the cell located between the pole pieces. This approximation is very useful in trying to understand the changes in cell voltage described in Chapter IV.

Another way in which an applied magnetic field can affect the cell voltage (or the related total cathode polarization) is presented and discussed by Mohanta and Fahidy (3,4) and Mohanta (5). The basic idea is that the apparent thickness of the diffusion layer is decreased by lateral sweeping of the electrode due to the increased convection currents, near the electrode's surface, associated with magnetohydrodynamic (MHD) effects.

Magnetoresistance. In (2) it is stated that the measured Hall constant associated with a given concentration of inorganic acid is much greater than the calculated value. The ratio of the observed value to the calculated value is approximately 5×10^5 to 1.

In (6), the following equation is given

$$\rho(B) = \rho(0)(1 + \mu^2 B^2). \tag{1-2}$$

Equation (1-2) gives the increase in magnetoresistance as a function of the applied $\vec{B}$ field, the mobility, μ, of the charge carrier and the initial resistivity, ρ_0. It should be noted that equation (1-2) is only valid for the case in which the Hall voltage is short circuited.

For the case in which a partial short circuit of the Hall voltage is present, the quadratic relation given in (1-2) is modified, and, finally, for the case in which there is no short circuit the magnetore-

sistance should be zero.

Substituting resistance for resistivity in equation (1-2) and solving for μ yields

(1-3) $$\mu = (R(B)/R(0) - 1)^{1/2}/B.$$

Finally, substituting in the experimental values given earlier (2), the result is

(1-4) $$\mu = [\frac{R(0) + R(0) \times (0.15)}{R(0)} - 1]^{1/2}(0.8 \text{ tesla})^{-1} .$$

The accepted value for the mobility of the H^+ ion is 3.5×10^{-7} m/sec per volt/m at 25°C. The ratio of this mobility to that given in equation (1-4) is 1.38×10^6 to 1.

Utilizing the relation $\sigma = ne\mu$, (6), and assuming that $\frac{1}{ne} \approx R_H$ (2), it follows that

(1-5) $$\frac{\mu}{\sigma} = \frac{1}{ne} \approx R_H.$$

In this expression σ is the conductivity, n is the number of charge carriers available per unit volume, e is the charge associated with each charge carrier and R_H is the Hall coefficient.

The equation, $\frac{1}{ne} \approx R_H$, is based on the idea that the mobility of the species of charge carriers of interest is much greater than that of the others, while the number of charge carriers of the various species is of the same order of magnitude.

Based on equation (1-5), along with the assumption that σ is roughly the same for both values of μ, one would expect R_H (observed) /R_H(calculated), i.e. 5×10^5, (2) to be roughly equal to the ratio of μ(observed)/μ(book value). This is indeed the case considering the approximations inherent in the determination of these two ratios.

The important point, associated with the above, is that the observed magnetoresistance should be much greater than the value expected based on the book value of μ_H^+. In fact, from equation (1-2) the expected increase in the resistance would be less than one part in 10^{13}, utilizing the book value of μ_H^+, while the observed increase is 15 parts per hundred.

That is, the observed magnetoresistance is roughly 10^{12} times greater than the expected value based on the book value of μ_H^+.

So far the discussion has centered around the idea that the magnetoresistance is much greater than would be expected. At this point the effect of pH on magnetoresistance should be considered. In (2), the following relation is given

(1-6) $$pH = a + b \log R_H.$$

For H_2SO_4 the experimental value of b is approximately 1 as would be expected from equation (1-5), that is, R_H decreases by a factor of 10 for each unit of pH drop.

There are several other factors which may effect the observed magnetoresistance. What may be one of the more important of these is the amount of stirring associated with the applied $\vec{B}$ field. If this stirring action is viewed as a means of internally short circuiting the Hall voltage, then one would expect that the greater the stirring action the greater the applicability of equation (1-2).

Even if the same cell configuration and applied magnetic field were utilized in each experiment there would still be several important variables to consider in determining the magnitude of this stirring effect. Among these are the current density, the viscosity of the

electrolyte, and the various ion species present in conjunction with their concentrations, transport numbers and mobilities.

Thermomagnetoelectric Effects. In (7) there is presented a considerable volume of data, which was collected with an electrolytic cell of the following dimensions: X = 80 mm, Y = 20 mm and Z = 1, 2, 3, or 4 mm. A constant magnetic field of 0.5 tesla was applied in the z direction by a permanent magnet. The applied electric field was either parallel or antiparallel to the positive x direction and the direction of the cell current was reversed several times during the coarse of each run. A schematic diagram of the cell indicating its general orientation is shown in Figure 1. (Note that the positive x direction is upward.)

The electrodes were located outside of the magnetic field and the temperature measurements were taken between the electrodes, within the uniform magnetic field. The temperature readings were taken parallel to the y axis at positions S_2 (y = Y/2) and S_1 (y = -Y/2). After these temperatures had stabilized they were recorded and the direction of cell current was reversed. Then, after the two temperatures had restabilized they were recorded once more.

Under the experimental conditions imposed in reference (7), (e.g. cell current always less than 60 ma, fairly dilute solutions, cell relatively narrow in the z direction, etc.), the magnitude of the change in temperature at Y/2 was equal to the magnitude of the change in temperature observed at -Y/2; however, the sign of the temperature change was reversed.

The following characteristics of the thermomagetoelectric effect

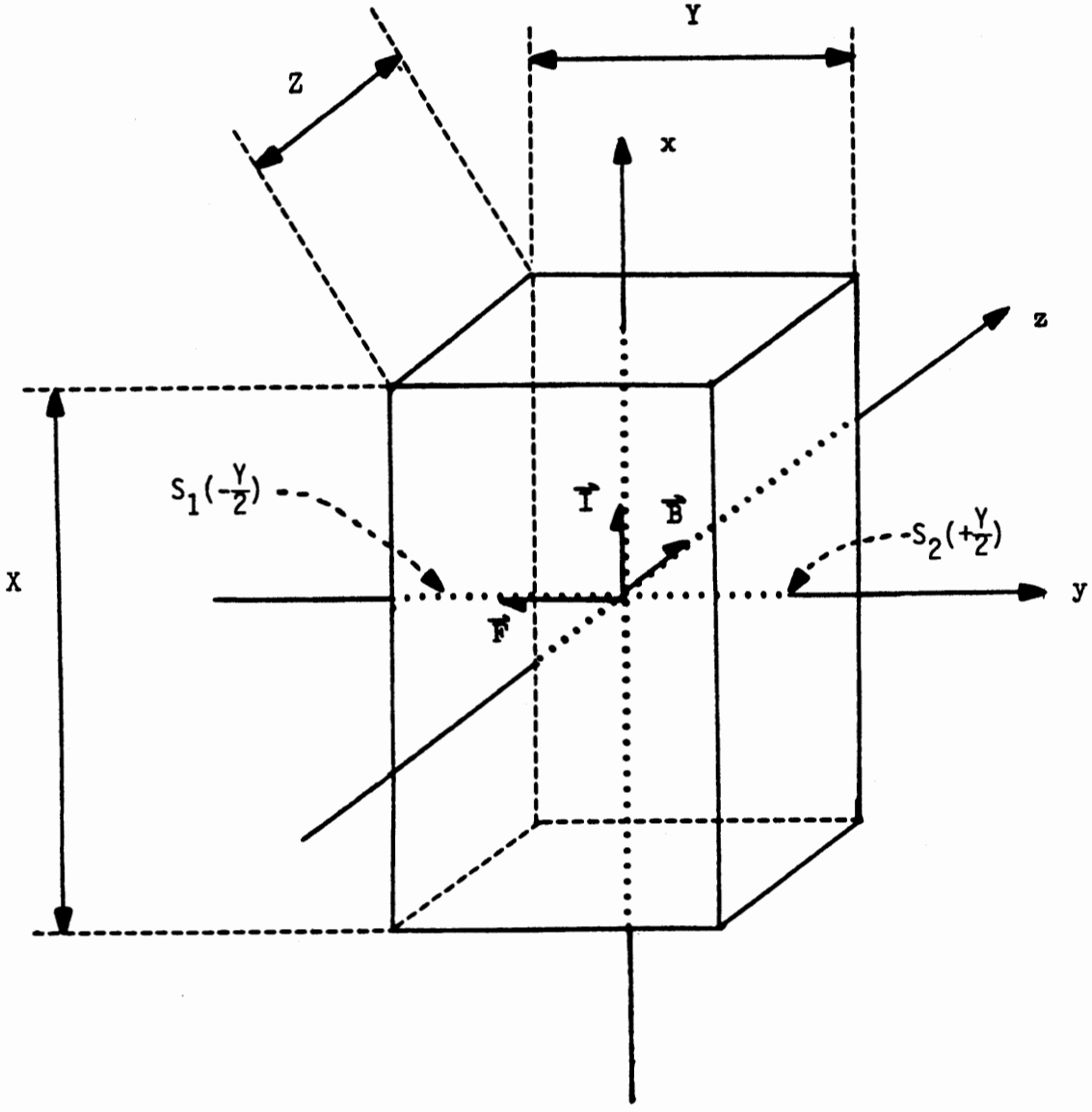

Figure 1. Position of the liquid sample, about the axis Ox, Oy, Oz for related work completed on the thermomagnetoelectric effect (7). $\vec{I}$: electrolysis current; $\vec{B}$: magnetic induction; $\vec{F}$: Lorentz force; X, Y, Z: dimensions of the cell.

are quoted from (7):

1) The heating effect is always in the direction of the magnetoelectric (Lorentz) force.
2) The variations in $\Delta T_s^{\infty} = T_s^{(+I)} - T_s^{(-I)}$ obtained for one of the thermocouples is equal and opposite to that given by the other thermocouple....
3) ΔT_s^{∞} increases when the electrolysis current increases.
4) ΔT_s^{∞} increases when the concentration decreases.
5) ΔT_s^{∞} decreases as the thickness of the cell increases.

In the above, $T_s^{(+I)}$ is the temperature observed for current flowing in the positive x direction and $T_s^{(-I)}$ is the observed temperature for current flow in the negative x direction. ΔT_s^{∞} is the difference between these two.

It is further noted (7), that ΔT_s^{∞} is less for acids than for bases. Furthermore, ΔT_s^{∞} is much greater for salts than for either acids or bases. The theoretical background material presented in the various French articles (7, 8, 9, 10) was not well enough defined to permit calculation of any well defined values of ΔT_s^{∞} for those solutions used in our experiments.

Magnetohydrodynamics (MHD). In this section, some of the pertinent fundamentals of MHD will be discussed. Included in this discussion are some rather basic equations describing the effect of magnetic fields on the transport of mass, momentum and electric charge. Along with the above, some approximations are described which are pertinent to the interaction of aqueous electrolytes with magnetic fields.

The intent of this discussion is not to present a rigorous solution based on the fundamental equations, but rather, to show that an applied magnetic field can distort the normal velocity distribution and that convective transfer can have a significant effect on the mass

transport for a static or non-flow cell.

This discussion is based primarily on earlier work presented by S. Mohanta in his M.S. thesis (5).

For the purpose of this discussion, the electrolytic solution may be thought of as a mixture of ions and undissociated molecules, with the ions functioning as the charge carriers. Since the ions are electrically charged they are subjected to three distinct forces under the combined electric and magnetic fields. These three forces can be broken down as follows:

I. Due to the existing charge distribution, there exists a force represented by the electrostatic field, $\vec{E}_s$ (volts/m). In conjunction with this field there exist the following two properties:

   a) from Coulomb's Law,

   $$\nabla \times \vec{E}_s = 0.$$

   b) and from Guass's Law in conjunction with the electroneutrality condition

   $$\nabla \cdot \vec{E}_s = q/\varepsilon_0 = 0.$$

II. The second force is that associated with a charged particle passing through a region exposed to magnetic field, $\vec{B}$.

   For example, consider a particle of charge q and velocity $\vec{v}$ (m/sec) traversing this field, the force exerted due to the magnetic field is given by $q(\vec{v} \times \vec{B})$ (measured in joules).

III. The final force to be considered is that due to the induced electric field, $\vec{E}_i$, which is associated with a time varying magnetic field as follows:

$$\nabla \times \vec{E}_i = -\frac{\partial \vec{B}}{\partial t}.$$

The vector sum of these three forces,

(1-7) $$q(\vec{E}_s + \vec{E}_i + \vec{v} \times \vec{B}) = q(\vec{E} + \vec{v} \times \vec{B}),$$

is the total force and is commonly referred to as the Lorentz force.

Since the magnetic field exerts a force on any moving charged particle, some net MHD body force would be expected on the electrolyte as a whole.

If a unit volume of the electrolyte is considered, and the individual "charge forces" are summed up the MHD body force density is obtained (5). This density is given as $\vec{J} \times \vec{B}$, where $\vec{J}$ is the current density.

For example, if the current density is 800 amps/m^2 and the value of $\vec{B}$ is taken to be 1 tesla then the corresponding force density is 800 Newtons/m^3. (This is for the case in which $\vec{J}$ and $\vec{B}$ are perpendicular to each other, otherwise the magnitude associated with the cross product would be less.)

In comparison, the gravitational force density for a typical aqueous electrolyte is about 10,000 Newtons/m^3.

If the forces acting on the electrolyte are not uniform the preceding analysis does not apply.

The modified Navier-Stokes equation gives the resulting velocity field as follows:

(1-8) $$\rho_L \frac{d\vec{v}}{dt} = \vec{J} \times \vec{B} + \eta \nabla^2 \vec{v} - \nabla P.$$

In this equation, incompressibility has been assumed, ρ_L is the density of the electrolyte, η is the viscosity of the electrolyte and P

is the thermodynamic pressure. Furthermore, η has been assumed to be constant although this is probably not the case in the diffusion layer.

The significance of the cross product term, $\vec{J} \times \vec{B}$ in equation (1-8) is demonstrated in an example from reference (5) concerning the momentum balance on the electrode. In this example, the electrolytic cell is undergoing electrolysis with verticle electrodes.

Consider one of the electrodes and assume that the electrolysis is being carried out in the diffusion-controlled region and that the natural convection theory yields an adequate description of the mass transfer process. Then, the current density is a function of height. (Instead of being uniform over the entire electrode surface.)

If the current density used during electrolysis is not near the limiting density, then the local current densities at various distances from the bottom of the cathode and the anode are given respectively as:

(1-9) $$J_c(x) = 0.8\ J_{c,ave.}\ (\frac{x}{L})^{-1/5} \text{ and}$$

(1-10) $$J_a(x) = 0.8\ J_{a,ave.}\ (\frac{L-x}{L})^{-1/5}.$$

In equations (1-9) and (1-10), L is the height of the electrode and x is the vertical distance from the bottom of the electrode.

Similar equations were given for the case in which electrolysis is carried out near the limiting current density. These equations for the cathode and anode are given respectively as:

(1-11) $$J_c(x) = 0.75\ J_{c,ave.}\ (\frac{x}{L})^{-1/4} \text{ and}$$

(1-12) $$J_a(x) = 0.75\ J_{a,ave.}\ (\frac{L-x}{L})^{-1/4}.$$

From equations 1-9 through 1-12, it can be seen that the current density is least uniform near the limiting density. This is made readily apparent by considering the integrals

$$I_c\Big|_{x_1}^{x_2} = \int_{x_1}^{x_2} J_c(x)dx = 0.8\ J_{c,\ ave.} \int_{x_1}^{x_2} \left(\frac{x}{L}\right)^{-1/5} dx = J_{c,\ ave.} \left(Lx^4\right)^{1/5}\Big|_{x_1}^{x_2} \text{ and}$$

$$I_c\Big|_{x_1}^{x_2} = \int_{x_1}^{x_2} J_c(x)dx = 0.75\ J_{c,\ ave.} \int_{x_1}^{x_2} \left(\frac{x}{L}\right)^{-1/4} dx = J_{c,\ ave.} \left(Lx^3\right)^{1/4}\Big|_{x_1}^{x_2}.$$

and recognizing that both equations may be rewritten in the form

(1-13) $$I_c\Big|_{x_1}^{x_2} = c_1 x^{4/5}\Big|_{x_1}^{x_2} \text{ and}$$

(1-14) $$I_c\Big|_{x_1}^{x_2} = c_2 x^{3/4}\Big|_{x_1}^{x_2}.$$

In the above equations c_1 and c_2 are constants and x_1 and x_2 are arbitrary values of x. Note, that the smaller the exponent in equations (1-13) and (1-14) the greater the weighting value placed on the smaller values of x.

From this point on, the discussion shall be limited to those current densities near the limiting densities.

For example, consider a cathode of width b, taking the center of the exposed area of the cathode as a reference point and assigning to the corresponding height the value of L/2 and choosing horizontal strips of width ΔS a distance S above and below this level, the corresponding magnitudes of the current densities are given respectively as:

(1-15) $$J_A = 0.75\ J_{c,ave.} \left(\frac{L/2 + S}{L}\right)^{-1/4} \text{ and}$$

(1-16) $$J_B = 0.75\ J_{c,ave.} \left(\frac{L/2 - S}{L}\right)^{-1/4}.$$

It should be noted that equations (1-15) and (1-16) are only valid for small magnetic fields. The reason for this is that sufficiently large fields would cause convection currents large enough to significantly alter the initial conditions.

The magnetic force per unit length (of the current filament), denoted by $\vec{P}_A$ and $\vec{P}_B$ are given by $\vec{J}_A \times \vec{B}$ and $\vec{J}_B \times \vec{B}$ respectively or

(1-17) $$P_A = 0.75\ J_{c,ave.}\ \left(\frac{L/2 + S}{L}\right)^{-1/4} BbΔS(N/m) \text{ and}$$

(1-18) $$P_B = 0.75\ J_{c,ave.}\ \left(\frac{L/2 - S}{L}\right)^{-1/4} BbΔS(N/m).$$

The corresponding torque, based on equations (1-17) and (1-18), is

$$0.75\ J_{c,ave.}\ Bb\ \left[\left(\frac{L/2 - S}{L}\right)^{-1/4} - \left(\frac{L/2 + S}{L}\right)^{-1/4}\right]SΔS(N\cdot m/m),$$

upon replacement of ΔS by dS and integrating one obtains

$$0.0726\ J_{c,ave.}\ BbL^2(N\cdot m/m)$$

for the torque per unit length.

Associated with this torque, movement of the electrolyte in the vicinity of the cathode is expected; a similar situation occurs for the anode.

CHAPTER II

EXPERIMENTAL METHODS

In this chapter, a general description of the experimental setup employed in the experiments discussed in Chapters III and IV is provided. Included in this description is a brief overview of the Rockwell R6500 Advanced Interactive Microcomputer, referred to as the AIM 65. Following this is a general description of the remaining experimental apparatus, including the manner in which the apparatus was arranged.

AIM 65 MICROCOMPUTER

The AIM 65 is a complete general purpose microcomputer (11) that can serve as a controller/monitor or a central processor.

The AIM 65 consists of two primary modules. These are the master module and the keyboard module. Included in the master module are the microcomputer components, a 20 column thermal printer and a 20 digit LED display. Both the printer and the display are able to produce the full 64 character ASC II set.

The ASC II code system and character set is based on the pairs of numbers obtained from all possible combinations of the two sets of numbers 0000 to 1111 and 000 to 111. (In this case, the order of the number pairs is set by convention.) Both of the sets of numbers are expressed in binary code and only one half of the combinations obtained are represented as printable characters on the standard (limited-ASC

II) keyboard. That is, there are 64 printable characters.

The heart of the AIM 65 is a fairly popular 8 bit-microprocessor, the R6502 Central Processing Unit (CPU). The R6502 is able to address 20K bytes of Read Only Memory, ROM, and 4K bytes of Random Access Memory, RAM, on the master module. In addition, it is able to address 40K bytes of ROM, RAM or Input/Output (I/O) externally. Its minimum execution time is 2 microseconds and it is capable of processing 56 different instructions in conjunction with 13 addressing modes (11).

Some of the other devices, which make up the AIM 65, are the R2114 RAM, the R2322 ROM, the R6532 RAM-I/O (RIOT), the R6532 Versatile Interface Adapter (VIA), and the R6520 Peripheral Interface Adapter (PIA).

A full-size 54 key, 70 function keyboard is included in the keyboard module. The keyboard functions are broken down as follows: (a) 26 alphabetic, (b) 10 numeric, (c) 22 special, (d) 9 control, and (e) 3 user defined.

A ROM-resident 8 K monitor controls the AIM 65 utilizing a comprehensive set of single key stroke commands. Quoting from reference (11), the Monitor includes commands to:

> Enter R6502 instructions in mnemonic form for direct translation to object code.
> Disassemble R6502 instructions from object code to mnemonic form.
> Execute user written programs with debugging aids such as instruction trace, register trace, and breakpoints.
> Display and alter memory and registers.
> Transfer object code to and from one or two audio cassette recorders or a teletype.
> Allow user-defined functions to interface with user-provided peripherals.

There are two basic models of the AIM 65 available, namely the 1K

RAM model and the 4K RAM model. Both of these models can be expanded by adding additional RAM, ROM, Programmable ROM(PROM), I/O and other peripheral chips. This is accomplished by extending the various bus lines to an expansion connector.

In our case, the AIM 65 had a total of 11758 bytes of available RAM.

The AIM 65 is interfaced to external equipment by utilizing the R6522 VIA in connection with an application connector. The VIA is equipped with two timers, four control lines, and 16 bi-directional I/O lines. The AIM 65 utilized for this research was equipped with two VIA's.

The program, which was used for data collection during those experiments in which the constant current mode was employed, is given in the appendix.

The purpose of this program was to collect and process various voltage values obtained from the 8800A-02 Fluke Digital Multimeter (8800A-02 DMM) by means of a built-in Data Output Unit, DOU. The DOU allowed two way communication between the AIM 65 and the 8800A-02 DMM.

By utilizing the appropriate probes, it was possible to monitor a number of different quantities. Among those were the cell temperature, cell current, cell voltage and the total amount of charge passed. All of the above were caculated from the corresponding voltages, in combination with the appropriate program steps and the AIM 65's internal clock.

Similar programs were utilized during the other experiments. The main difference, between the various programs, was in the number and

types of probes monitored. In some of the experiments addtional quantities such as pH were measured, while in others the variety was more restricted in nature.

EXPERIMENTAL SETUP

The general experimental setup is shown in Figure 2. The primary electrolysis circuit is indicated by the dashed lines while the remaining circuit is drawn in with solid lines.

For all of the experimental work conducted in this research the same basic setup was utilized, the primary variable being the actual electrolysis cell used. The various electrolytic cells are described in detail in Chapters III and IV.

For the electrolysis experiments discussed in Chapter III only one electrode was placed between the pole pieces and that was the electrode nearest the rear of the electromagnet. In all of these experiments the two-inch pole pieces were used.

For most of the experiments discussed in Chapter IV the four-inch pole pieces were used. When this was the case the electrode nearest the front of the electromagnet was located between the pole pieces. In contrast with this in some experiments both electrodes were placed between the pole pieces. For those experiments in which the two-inch pole pieces were used, the anode was located nearest the rear of the electromagnet and was positioned between the pole pieces.

Generally, for those experiments discussed in Chapters III and IV the cell voltage was measured between the two electrodes, C, while the cell current was calculated based on the voltage drop measured across

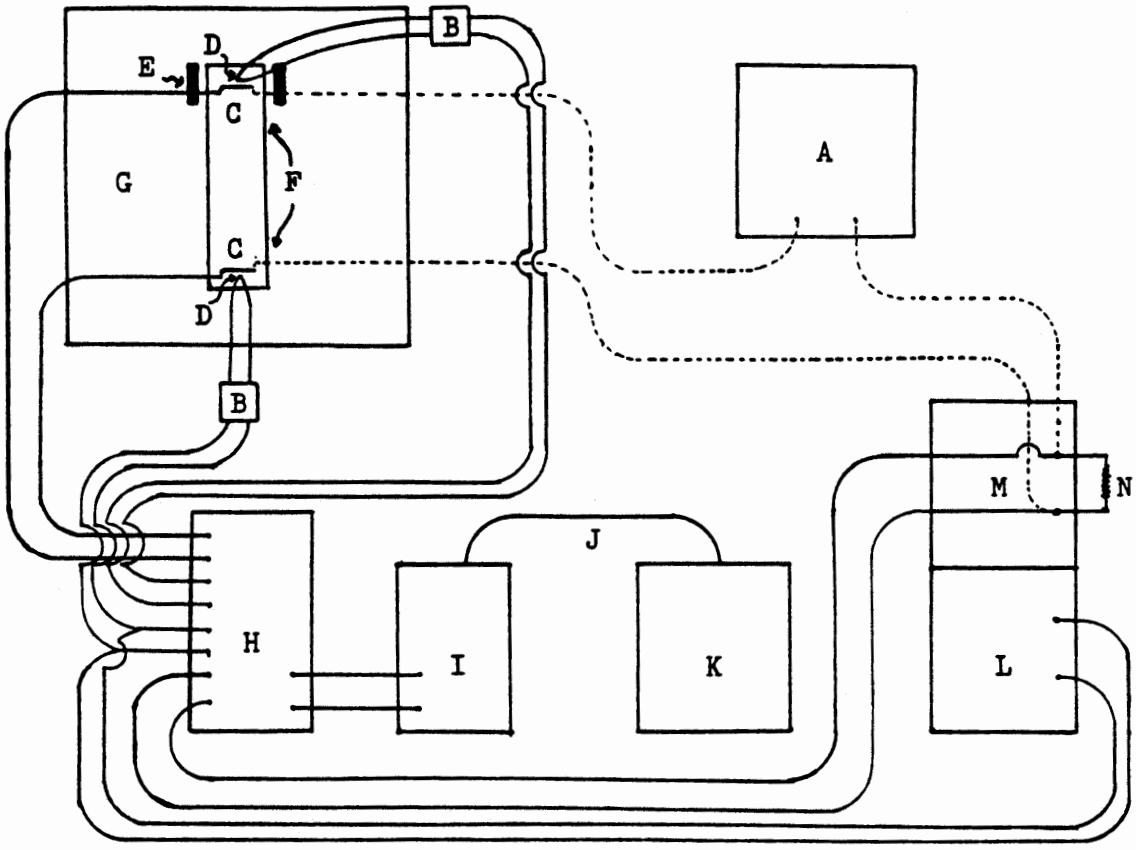

Figure 2. General experimental setup. The letters used in this diagram are defined as follows:

A. Hewlett Packard DC Power Supply, Model 6202B.
B. Omega Electronic Ice Point, Model MCJ.
C. Electrolysis electrode.
D. Chromel-alumel thermocouple.
E. Pole pieces.
F. Electrolysis cell.
G. Varian electromagnet, Model V-4004.
H. Switching mechanism.
I. Fluke Digital Multimeter equipped with DOU (Data Output Unit), Model 8800A-02
J. Bus line connecting DOU (from the digital multimeter) to the AIM 65 Microcomputer.
K. AIM 65 Microcomputer.
L. Houston Instrument, Omnigraphic strip chart recorder, Model 3000, channel 1.
M. Houston Instrument, Omnigraphic strip chart recorder, Model 3000, channel 2.
N. International Resistance Company, precision wire wound resistor, 0.1 Ohm +/- 1%.

N. Included in the latter calculation was a correction factor for the resistance associated with the required leads. The total charge passed was calculated from the measured values of the cell current in conjunction with the appropriate time intervals measured by the AIM 65's internal clock.

The various temperature measurements were obtained by utilizing the potential difference provided by the combination of one of the thermocouples, D, and the corresponding electronic ice point, B. From this potential difference the temperature was obtained.

For all of the electrolytic solutions discussed in Chapters III and IV the solvent used was deionized H_2O, with a resistivity of 17 megohms-cm.

All measurements of the $\vec{B}$ field were taken with a Bell Gaussmeter (Model 620).

CHAPTER III

EFFECTS OF MAGNETIC FIELDS ON THE ELECTROLYSIS OF WATER

In this chapter, several effects associated with magnetic fields are introduced and discussed in some detail. The primary effects discussed are related to the rates of collection of H_2 and O_2 and to the changes in temperature noted just above each of the two electrodes, as well as, temperature changes observed between the two electrodes.

In all of the runs discussed in this section, the strength of the applied magnetic field was 1.1 tesla as measured between the pole pieces when the electromagnet was energized, in either the normal or reverse modes. When the magnet current was turned off the residual magnetic field was 0.014 to 0.015 tesla and was in the same direction as that associated with the preceeding energized mode.

The variation of the $\vec{B}$ field as a function of distance from the center of the pole pieces is shown in Figure 3. Since the other electrode was slightly under 30 cm away it was exposed to an applied magnetic field of 0.002 tesla when the electromagnet was turned on.

The actual cell used to observe these phenomena is shown in Figure 4. The entire bottom half of the cell (which excludes just the central reservoir along with its integral connecting tube and the two gas collecting tubes) was insulated with Pyrex glass wool and for those experiments in which no gas collection was attempted just the bottom half of the cell was used. The electrodes were made of corrugated

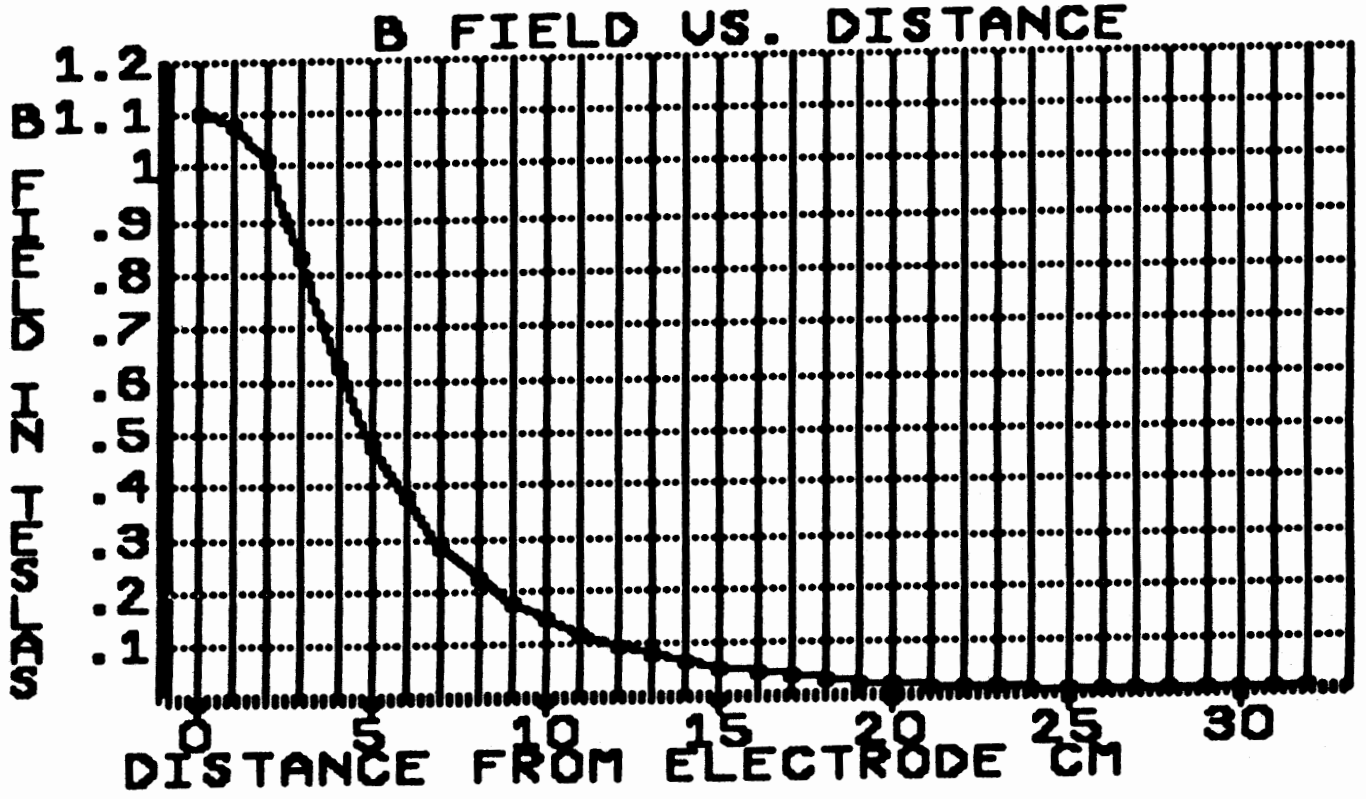

Figure 3. Applied magnetic field as a function of distance. This figure is based on a magnet current of 4.0 amperes and 2 inch diameter pole pieces. The gap between the pole pieces was approximately 2.8 cm.

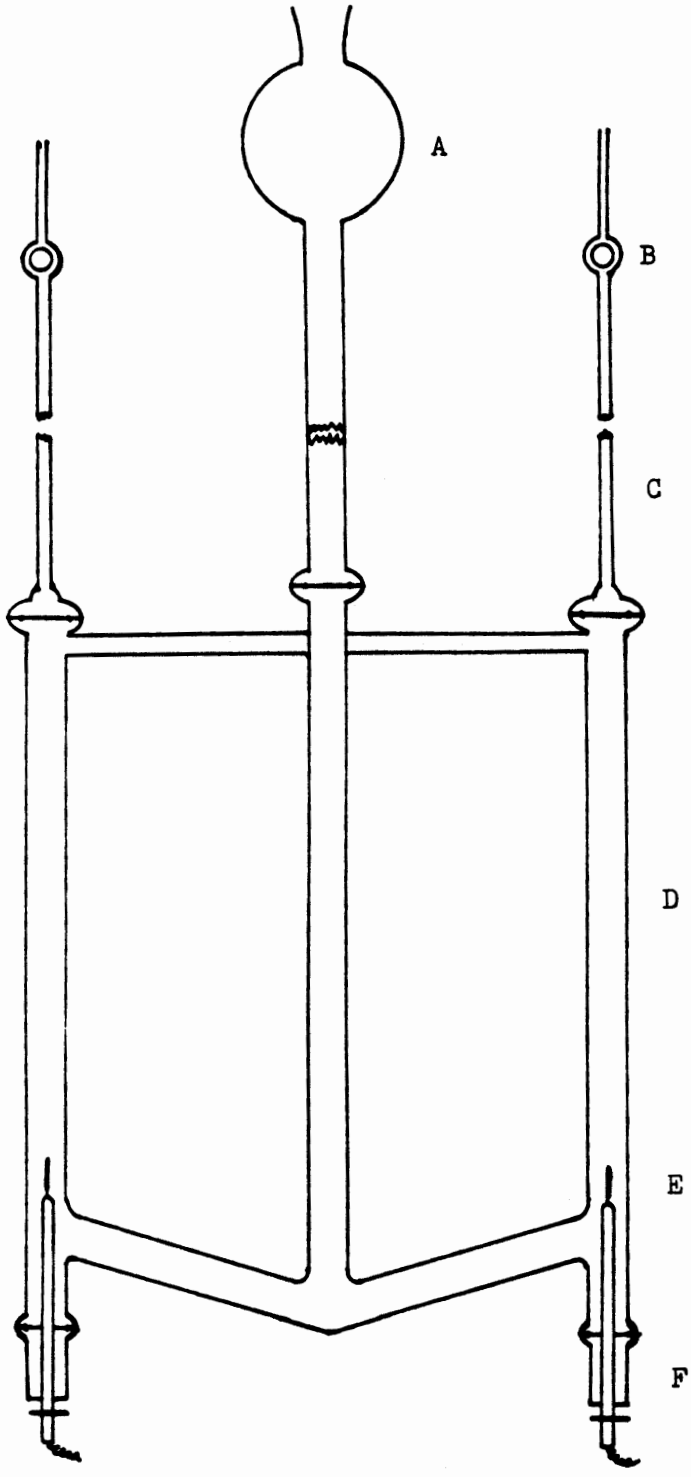

SCALE:

1 CM = 3.8 CM

Figure 4. Primary cell used during the electrolysis of water experiments. The labeled components are as follows: (A) central reservoir, (B) ground glass stopcock, (C) gas collecting tube, (D) main cell body, (E) platinum electrode and (F) Lexan electrode holder. Components A through D were made of Pyrex.

platinum and were 5.65 mm ± 0.05 mm wide by 19.7 mm ± 0.2 mm long by approximately 0.02 mm thick.

The corrugation increases the measured width by approximately 3.5% so the total gross surface area was about 2.30 cm^2 ± 0.05 cm^2. Furthermore, it should be noted that in all cases either the H_2 or the O_2 electrode was located between the pole pieces of the electromagnet.

The electrolysis cell was bilaterally symmetrical about two mutally orthogonal planes. One of these planes is that illustrated in Figure 4. The other plane is perpendicular to the page and contains the central axis of the tube leading up to the central reservoir.

If one defines the direction of the $\vec{B}$ field as being along the z axis, for a normal magnetic field orientation, and the increasing vertical direction as the y axis, then the positve x direction is envisioned as coming out of the front of the electromagnet. (That is, in Figure 2, the positive x direction is in the plane of the paper and pointing towards the bottom of the page.) This general orientation is shown diagrammatically in Figure 5.

In all of the experiments discussed in this chapter, the applied magnetic field was oriented parallel to either the positive (referred to as the normal magnetic field orientation) or the negative z direction (referred to as the reverse magnetic field orientation).

The electrolyte utilized during the electrolysis of water experiments was made up of a mixture of deionized H_2O and reagent grade H_2SO_4. The concentration of sulfuric acid was 50 ml per liter of solution for the runs of 8/6/81 and 8/17/81 and 175 ml per liter of solution for the runs of 8/24/81 through 8/26/81.

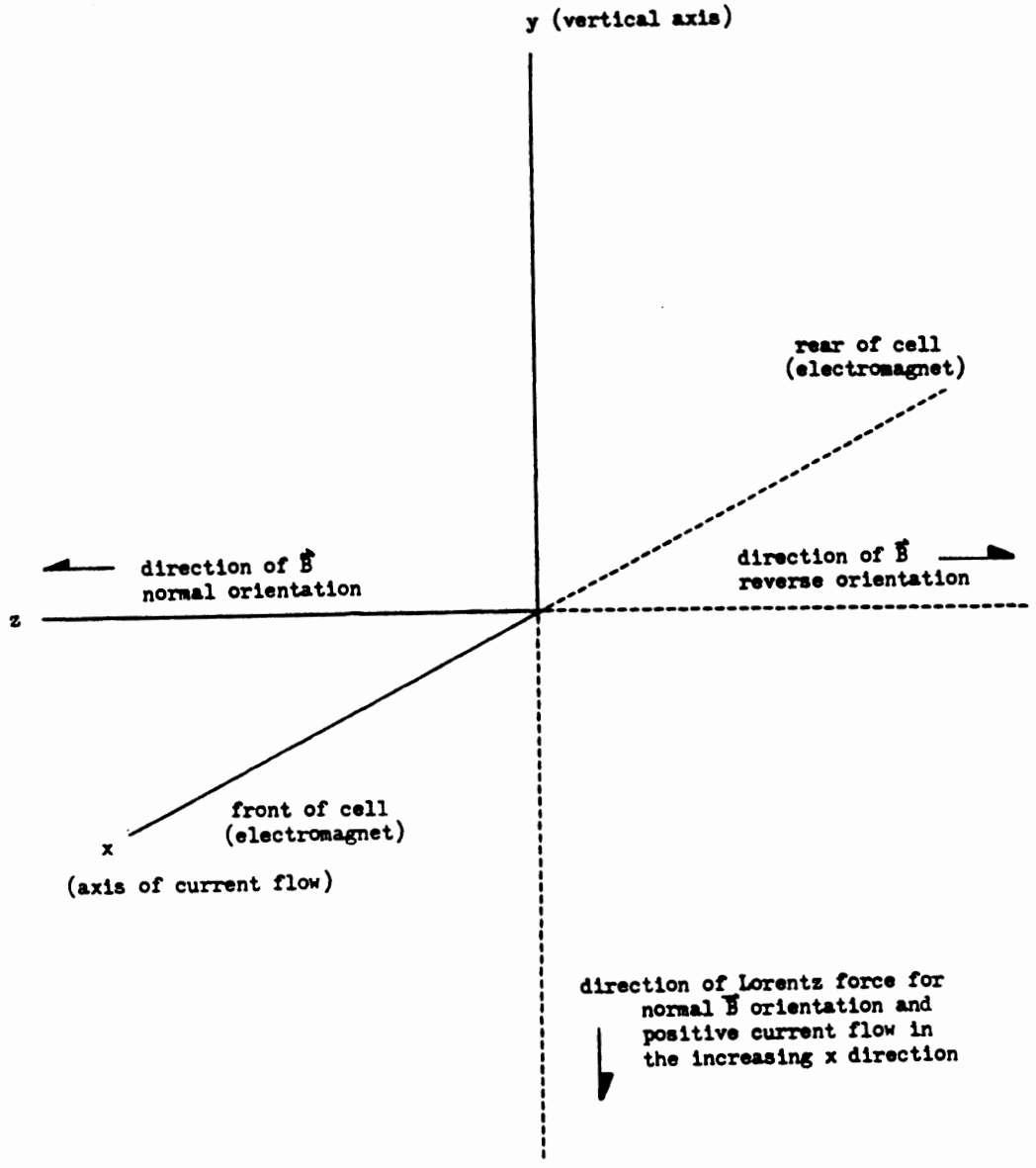

Figure 5. Basic cell orientation for the experiments discussed in Chapters III and IV. Note, that for the cell shown in Figure 4, the current path is along the x-axis near the center of the cell, otherwise the deviation is approximately 15° due to the cell configuration.

The specific experimental details, aside from those mentioned in Chapter II or the preceeding portion of this chapter, will be brought out in the following analysis on a section by section basis.

EFFECTS ON GAS PRODUCTION AND COLLECTION

In this section, the primary subject of discussion is the effect of magnetic fields on the production and collection of H_2 and O_2.

The first point to consider is the total amount of H_2 and O_2 collected during a given run or series of runs using a given experimental setup. These totals are compared to the theoretical values, which were calculated based on the number of coulombs passed. Finally, from the ratios of the experimental to the theoretical values, the overall effect of the magnetic field on the total volume of O_2 and H_2 collected is determined.

In Table I, the total gas volumes actually observed on the H_2 and O_2 sides of the cell are provided for each individual run. Each run is composed of a series of segments in which the magnet current was alternately turned on and off. For those runs conducted on 8/6/81 and 8/17/81 the total length of each run was a minimum of 40 minutes and each one of the segments was 10 minutes long. Similarly for the runs of 8/24/81 through 8/26/81 the overall length of the runs was a minimum of 15 minutes and the magnet current was switched every 3 minutes.

For all of the gas collection experiments, the constant voltage mode was utilized. That is, the cell current was the variable quantity.

For the 40 minute runs, the cell voltage was in the range of

TABLE I

TOTAL GAS VOLUMES OBSERVED ON THE H_2 AND O_2 SIDES OF THE WATER ELECTROLYSIS CELL

Date	Run Number	Measured Volume O_2(ml)	Measured Volume H_2(ml)	Mean Cell Temperature (°C)
8/6/81	1	23.12	48.90	21.51
	2	24.39	49.55	22.03
	3	24.60	50.30	22.08
	4	24.75	50.40	22.69
8/17/81	1	23.70	50.30	23.38
	2	25.80	52.24	23.52
	3	25.52	51.59	23.87
	4	25.46	51.22	23.86
8/24/81	1 of series 1	22.35	44.31	24.83
	2 of series 1	22.60	44.22	25.11
	3 of series 1	22.60	44.42	25.54
	4 of series 1	22.60	44.30	25.77
	1 of series 2	22.35	43.83	24.86
	2 of series 2	22.43	44.01	25.46
	3 of series 2	22.40	43.91	25.77
8/25/81	1 of series 1	21.30	44.98	23.77
	2 of series 1	22.48	44.19	25.10
	3 of series 1	22.72	44.68	25.62
	4 of series 1	22.72	44.85	25.93
	1 of series 2	22.60	44.62	25.96
	2 of series 2	22.63	44.50	26.13
	3 of series 2	22.70	44.85	26.16
	4 of series 2	22.70	44.75	26.29
8/26/81	1	22.80	45.15	24.90
	2	23.45	45.70	26.87
	3	23.35	45.80	27.72
	4	23.10	45.50	27.62

8.9780 to 8.9930 volts and similarly for the 15 minute runs the cell voltage was in the range of 9.0250 to 9.0345 volts. Furthermore, for any given series of runs the maximum variation in cell voltage was 0.0065 volts or less and typically the variation in cell voltage for any given run was less than 0.0025 volts (that is less than 0.03% of the total cell voltage).

The cell for the gas collection experiments (Figure 4) was made up of a large primary cell (constructed of Pyrex glass) with various component parts attached to it.

In every case, where a component part was attached to the main cell, viton 'o' rings in conjunction with the appropriate 'o' ring joints and clamps were used.

The body of the electrode holder was made of Lexan plastic. While the internal parts of the holder consisted of two small viton 'o' rings along with two cylindrical pieces of Lexan. At the bottom of the electrode holder there was, what was essentially, a hollow bolt machined out of Lexan. When this hollow bolt was screwed in, the two cylindrical pieces of Lexan pushed against the viton 'o' rings. These, in turn, sealed around a small glass tube which contained the lead going to the platinum electrode.

Prior to each run, the stopcocks were opened and any accumulated gas was released. During the course of the run, the gas volumes were recorded each time the magnetic field was changed; however, the gas volume was allowed to accumulate over the entire course of each run.

At this point, the discussion is restricted to the total gas volumes collected during the course of each run. However, later on in

this chapter, the discussion will focus on the individual volume measurements conducted for each individual run segment.

Consider that the total gas volumes collected during the individual runs have been recorded. At this point, there are several corrections which must be made. These corrections are required because of increases in pressure associated with increasing gas volumes, along with temperature and room pressure variations. In addition, it is necessary to correct for the vapor pressure of the electrolyte.

The above corrections are accomplished in two separate steps. The first one takes into consideration all of the above factors except for the vapor pressure of the electrolyte, which is taken care of in step number two.

In order to complete the first step in the correction process the following two equations were utilized for concentrations of 50 ml H_2SO_4/liter and 175 ml H_2SO_4/liter respectively:

(3-1)

$$V_c = (T_o/T_m)(V_m)[P_m/P_o + V_m(1.119 \times 10^{-3}/ml) + 0.0026]$$

$$\text{and } V_c = (T_o/T_m)(V_m)[P_m/P_o + V_m(1.256 \times 10^{-3}/ml) + 0.0026]$$

In the above equations, T_m, V_m, and P_m are the measured values of the cell temperature (in °K), the total gas volume (measured in ml on either the H_2 or O_2 side), and the measured room atmospheric pressure, respectively.

Similarly, T_o, P_o, and V_c are respectively 298.15°K, standard atmospheric pressure, and the volume (in ml) occupied by the gas at T_o and P_o.

To demonstrate the development of equations (3-1), the derivation

of the first of these equations is presented at this time.

Examining the calibrated gas collecting tubes shown in Figure 4, it was determined that for the central portion of the tube a volume change of 45 ml corresponds to a change of height in the liquid-gas interface of 49.30 cm ± 0.01 cm.

In MKS units the value of P_o is 101325 N/m^2. If we assume the density of water is 0.997 g/cm^3 (i.e. the approximate density of H_2O at 25°C) and the specific gravity of the sulfuric acid is 1.84, then the density of the electrolyte is given as follows:

$$[(966 \text{ ml } H_2O)(0.997 \text{ g/cm}^3) + (50 \text{ ml } H_2SO_4)(1.84 \text{ g/cm}^3)]/1000 \text{ ml} = 1.055 \text{ g/cm}^3.$$

Note, that H_2SO_4 is soluble in H_2O. For this reason 966 ml of H_2O was required to make a liter of electrolyte instead of the expected 950 ml. (The required volume of H_2O was determined experimentally.)

Utilizing Newton's second law of motion the following relation is obtained:

$$P_o = \left(\frac{\text{mass}}{\text{area}}\right)g \rightarrow \frac{\text{mass}}{\text{area}} = 1.0333 \times 10^3 \text{ g/cm}^2.$$

From the above, it follows that the column height, C, required to increase the internal pressure by 1 atmosphere is given by

(3-2) $$C = (\text{mass/area})/(\text{density of electrolyte})$$
$$(1033.3 \text{ g/cm}^2)/(1.055 \text{ g/cm}^3) = 979 \text{ cm}.$$

Now, from the ideal gas law, PV = nRT, therefore

(3-3) $$P_1V_m/T_m = P_oV_c/T_o,$$

where P_1 is the pressure inside the gas collecting tube.

If we let H = actual height of the liquid column (head) in cm then:

$$P_1 = P_o(P_m/P_o + H/C); \quad H = V_m(49.30 \text{ cm})/(45.00 \text{ ml}) = V_m(1.0956 \text{ cm/ml})$$

$$\rightarrow V_c = (P_1V_m/T_m)(T_o/P_o) = (V_mP_o/P_o)[P_m/P_o + V_m(1.0956 \text{ cm/ml})/C](T_o/T_m).$$

or upon substituting in the value of C, from equation (3-2) and simplifying somewhat,

(3-4) $V_C=(T_o/T_m)(V_m)[P_m/P_o + V_m(1.119 \times 10^{-3}/ml)+0.0026]$

The last term of 0.0026, (2.5 cm/979 cm), was added to take into account the fact that there was an increase of about 2.5 cm ± 0.2 cm in the electrolyte level of the central reservoir over the course of each run.

The second part of equation (3-1) was obtained in an identical manner except for the fact that the density of the electrolyte was now 1.185 g/cm^3. Once again the amount of water required was more than might be expected (866 ml compared to 825 ml).

The above density of 1.185 g/cm^3 implies that C is equal to 872 cm. From this the second part of equation (3-1) follows directly, as given below.

(3-5) $V_C=(T_o/T_m)(V_m)[P_m/P_o + V_m(1.256 \times 10^{-3}/ml)+0.0026]$

In this case, the last term of 0.0026 remains essentially the same. Since the change in the reservoir level was approximately 2.3 cm ± 0.2 cm.

The room atmospheric pressure, for those days on which experiments were conducted, is given in Table II.

TABLE II

ROOM ATMOSPHERIC PRESSURE
DURING GAS COLLECTION
EXPERIMENTS

Date	Lowest Pressure (in Hg)	Highest Pressure (in Hg)	Average pressure (in Hg)
8/5/81	30.085	30.130	30.108
8/5/81	30.055	30.085	30.070
8/17/81	29.850	29.900	29.875
8/24/81	29.925	29.940	29.933
8/25/81	30.095	30.100	30.098
8/26/81	30.125	30.135	30.130

Using the average atmospheric pressure, in conjunction with Table I and equation (3-1), Table III follows directly.

We have computed the total volume which was actually present on each side of the cell; the next step is to compute what proportion of the measured volume is associated with the vapor pressure of the electrolyte.

From reference (12), we have, $\Delta P = P^0 N_2$. In this equation N_2 is the mol fraction of solute, P^0 is the vapor pressure of pure solvent (H_2O in this case) and ΔP is the extent of vapor pressure lowering. The preceeding equation is only valid for solutions of nonelectrolytes. For electrolytic solutions, this must be modified slightly and is given as follows:

(3-6) $$\Delta P = iP^0 N_2$$

In which, i is the van't Hoff factor. The van't Hoff factor is defined as the ratio of the colligative effect produced by a concentration, m, of electrolyte divided by the effect observed for the same concentration of nonelectrolyte. The colligative properties include vapor pressure lowering, boiling point elevation, and freezing point

TABLE III

OBSERVED GAS VOLUMES COLLECTED
CORRECTED FOR TEMPERATURE AND
PRIMARY PRESSURE EFFECTS

Date	Run Number	Electrode between Pole Pieces	Volume O_2(ml)	Volume H_2(ml)
8/6/81	1	Hydrogen	24.18	52.56
	2	Hydrogen	25.49	53.20
	3	Hydrogen	25.72	54.04
	4	Hydrogen	25.82	54.04
8/17/81	1	Hydrogen	24.49	53.47
	2	Hydrogen	26.70	55.62
	3	Hydrogen	26.38	54.83
	4	Hydrogen	26.31	54.42
8/24/81	1 of series 1	Hydrogen	23.06	46.94
	2 of series 1	Hydrogen	23.30	46.79
	3 of series 1	Hydrogen	23.27	46.95
	4 of series 1	Hydrogen	23.25	46.78
	1 of series 2	Hydrogen	23.06	46.40
	2 of series 2	Hydrogen	23.09	46.50
	3 of series 2	Hydrogen	23.04	46.34
8/25/81	1 of series 1	Oxygen	22.14	48.10
	2 of series 1	Oxygen	23.30	47.00
	3 of series 1	Oxygen	23.51	47.47
	4 of series 1	Oxygen	23.49	47.61
	1 of series 2	Oxygen	23.36	47.35
	2 of series 2	Oxygen	23.38	47.35
	3 of series 2	Oxygen	23.45	47.57
	4 of series 2	Oxygen	23.44	47.44
8/26/81	1	Hydrogen	23.68	48.16
	2	Hydrogen	24.21	48.46
	3	Hydrogen	24.04	48.43
	4	Hydrogen	23.78	48.11

lowering along with similar effects on the osmotic pressure. It should be noted, that, although it is necessary to determine i experimentally, once it is determined it is valid essentially for all of the colligative properties.

In our experiments, the solutions contained either 50 ml H_2SO_4/l or 175 ml H_2SO_4/l. ΔP is given as follows, for 50 ml H_2SO_4/l:

(3-7) $$\Delta P = iP^0[\ (W_2/M_2)/(W_1/M_1 + W_2/M_2)\ ] = 0.0172iP^0$$

In which, M_1 is the molecular weight of the solvent (deionized H_2O), W_1 is the actual mass of the solvent present per liter, and M_2 and W_2 are the molecular weight and actual mass of the solute (H_2SO_4) present. Similarly for 175 ml H_2SO_4/l:

(3-8) $$\Delta P = 0.0641iP^0$$

In reference (12), the values of i are given in terms of the molality of the solution. For 50 ml H_2SO_4/l the molality is

$$[(50\text{ ml } H_2SO_4 \times 1.84\text{ g/ml})/(98.08\text{ g/mole})]/(0.966\text{ l} \times 0.997\text{ Kg/l } H_2O$$

$$= 0.974\text{ g-mol } H_2SO_4/\text{Kg } H_2O.$$

Similarly, for 175 ml H_2SO_4/l the molality is given by:

$$[(175\text{ ml } H_2SO_4 \times 1.84\text{ g/ml})/(98.08\text{ g/mole})]/(0.866\text{ l} \times 0.997\text{ Kg/l } H_2O$$

$$= 3.802\text{ g-mol } H_2SO_4/\text{Kg } H_2O.$$

The corresponding values of i, obtained by linearly extrapolating between the values of i given in reference (12) are as follows:

For 50 ml H_2SO_4/liter: i = 2.16.

For 175 ml H_2SO_4/liter: i = 3.69.

Substituting these values of i into equations (3-7) and (3-8), respectively, yields:

(3-9) $$\Delta P = iP^0N_2 = (2.16)(P^0)(0.0172) = 0.0372P^0,$$

for 50 ml H_2SO_4/liter of solution. Similarly for 175 ml H_2SO_4/liter,

(3-10) $$\Delta P = iP^0N_2 = (3.69)(P^0)(0.0641) = 0.2365P^0.$$

Because the vapor pressure of water is dependent on temperature, the temperature of the electrolyte must be known with some accuracy. For the experiments discussed in this section, temperature measurements were conducted every 30 seconds. These temperature measurements were obtained in the central vertical tube approximately 1 cm above the top of the tube connecting the two sides of the cell. In this case, the average cell temperature for each run appears to be the most reasonable quantity to consider. This same quantity was utilized previously in the completion of Table III.

Based on the preceeding narrative, in conjunction with the vapor pressure of H_2O as given in reference (13), Table IV follows naturally.

Now, that the vapor pressure, $P^0-\Delta P$, has been determined, let us rename this term P_e and determine the manner in which this correction should be applied.

The vapor pressure is affected only slightly by the partial pressure of an indifferent gas (14). If we assume that this representation is valid in this case, then the most accurate way to correct for this vapor pressure is in terms of the measured volume, V_m. Assuming this to be the case, if the pressure in the gas collecting tube is expressed in the form $(V_c/V_m) \cdot 760$ mm Hg, where V_c is thecorrected gas volume discussed previously, then the decrease in the measured gas volume is given as

$$V_m[(P_e \cdot V_m)/(V_c \cdot 760 \text{ mm Hg})](T_o/T_m). \tag{3-11}$$

Therefore, the actual collected gas volume, V_a, is

$$V_a = V_c[V_m - V_m((T_o \cdot P_e \cdot V_m)/(T_m \cdot V_c \cdot 760 \text{ mm Hg}))]/V_m \tag{3-12}$$

TABLE IV

VAPOR PRESSURE OF THE ELECTROLYTIC SOLUTION

			Pressure in mm Hg		
Date	Run Number	Average Temp.(°C)	Vapor Pressure H_2O P^0	Change in Vapor Pressure ΔP	Vapor pressure H_2SO_4 Solution $P_e=(P^0-\Delta P)$
8/6/81	1	21.51	19.24	0.72	18.52
	2	22.03	19.86	0.74	19.12
	3	22.08	19.92	0.74	19.18
	4	22.69	20.68	0.77	19.91
8/17/81	1	23.38	21.56	0.80	20.76
	2	23.52	21.74	0.81	20.93
	3	23.87	22.20	0.83	21.37
	4	23.86	22.19	0.83	21.36
8/24/81	1 of series 1	24.83	23.52	5.56	17.96
	2 of series 1	25.11	23.91	5.65	18.26
	3 of series 1	25.54	24.53	5.80	18.73
	4 of series 1	25.77	24.87	5.88	18.99
8/24/81	1 of series 2	24.86	23.56	5.57	17.99
	2 of series 2	25.46	24.41	5.77	18.64
	3 of series 2	25.77	24.87	5.88	18.99
8/25/81	1 of series 1	23.77	22.07	5.22	16.85
	2 of series 1	25.10	23.90	5.65	18.25
	3 of series 1	25.62	24.65	5.83	18.82
	4 of series 1	25.93	25.11	5.94	19.17
8/25/81	1 of series 2	25.96	25.15	5.95	19.20
	2 of series 2	26.13	25.40	6.01	19.39
	3 of series 2	26.16	25.45	6.02	19.43
	4 of series 2	26.29	25.65	6.07	19.58
8/26/81	1	24.90	23.62	5.59	18.03
	2	26.87	26.54	6.28	20.26
	3	27.72	27.89	6.60	21.29
	4	27.62	27.73	6.56	21.17

or, after simplification

(3-13) $$V_a = V_c[1 - (T_o \cdot P_e \cdot V_m)/(T_m \cdot V_c \cdot 760 \text{ mm Hg})].$$

By the application of equation (3-13), in conjunction with Tables I, III and IV, the values of V_a, given in Table V, were obtained.

In reference (14) the assumption was made that none of the indifferent gas dissolves in the solution. This is not the case for either hydrogen or oxygen. What is interesting, however, is that for any given day after the first segment of the first run the solution should be fairly well saturated on both sides of the cell. Following this line of reasoning, the effects of increasing cell temperature and pressure in the various portions of the electrolyte seem to nearly cancel in terms of the net gas volume gained from or lost to the gas collecting tubes. The net effect being a few hundredths of a ml or less on either side of the cell over the course of a given run.

During the individual segments of a run these two effects may be relatively more important but they probably account for no more than 5 to 10% of the observed changes in the rate of gas accumulation associated with changing the applied magnetic field.

Now that the values of V_a are known, the next step is to compute the expected gas volumes based on the number of coulombs passed and to see how these values compare with the corresponding V_a values.

Based on van der Waals' equation,

(3-14) $$(P + a/V^2)(V - b) = RT,$$

and the values of a and b provided in reference (13), it follows that for T = 25°C and P = 1 atm, one mole of H_2 occupies a volume of 24.484 liters. Under similar conditions, one mole of O_2 occupies a volume of

TABLE V

ACTUAL GAS VOLUME COLLECTED AT
25°C AND ONE ATMOSPHERE

Date	Run Number	Electrode between Pole Pieces	Volume O_2(ml)	Volume H_2(ml)
8/6/81	1	Hydrogen	23.62	51.37
	2	Hydrogen	24.88	51.95
	3	Hydrogen	25.10	52.77
	4	Hydrogen	25.17	52.72
8/17/81	1	Hydrogen	23.84	52.10
	2	Hydrogen	25.99	54.18
	3	Hydrogen	25.66	53.38
	4	Hydrogen	25.59	52.98
8/24/81	1 of series 1	Hydrogen	22.54	45.92
	2 of series 1	Hydrogen	22.77	45.75
	3 of series 1	Hydrogen	22.72	45.88
	4 of series 1	Hydrogen	22.70	45.70
8/24/81	1 of series 2	Hydrogen	22.54	45.38
	2 of series 2	Hydrogen	22.55	45.44
	3 of series 2	Hydrogen	22.49	45.27
8/25/81	1 of series 1	Oxygen	21.68	47.12
	2 of series 1	Oxygen	22.77	45.96
	3 of series 1	Oxygen	22.96	46.39
	4 of series 1	Oxygen	22.93	46.50
8/25/81	1 of series 2	Oxygen	22.80	46.25
	2 of series 2	Oxygen	22.81	46.08
	3 of series 2	Oxygen	22.88	46.45
	4 of series 2	Oxygen	22.87	46.31
8/26/81	1	Hydrogen	23.15	47.11
	2	Hydrogen	23.60	47.27
	3	Hydrogen	23.40	47.17
	4	Hydrogen	23.15	46.87

24.443 liters.

Given the above, the next step is to determine the number of ml of gas produced per coulomb passed. For H_2, this is given as follows: (1.60219 x 10^{-19} coul/H^+ ion) x (2 H^+ ions/H_2 molecule) x (6.0227 x 10^{23} H_2 molecules/mole) x (1 mole/24.484 liters H_2) = 7.8819 x 10^3 coulombs/liter H_2 or 1.2688 x 10^{-1} ml H_2/coulomb passed. Preceding in a similar manner, the corresponding value for O_2 is obtained. This value is 6.3333 x 10^{-2} ml O_2/Coulomb passed.

Utilizing the preceding ratios, between coulombs passed and ml of gas produced along with the appropriate coulomb values obtained from the experimental data, the calculated volume of H_2 and O_2 were derived. This, in turn, made it possible to complete Table VI. If the preceding corrections to the total gas volumes are applied to the individual segments (for specific magnetic field orientations) and these results are plotted for the entire run, the results given in Figures 6, 7, 8, and 9 are obtained.

In these figures, there is one correction which has been neglected. This correction is the one associated with the rise in the level of the air-electrolyte interface in the central reservoir as the volume of collected gas increases. Over the course of each run, the lack of this correction, with respect to the measured gas volume on the hydrogen side of the cell leads to a total deficit of 0.12 ml ± 0.01 ml. For the oxygen side of the cell, the magnitude of this effect is approximately one half the above value.

The size of this effect increases over the course of each run. The rate of increase is not linear with respect to time; however, the rate should always be positive. For this reason the relative magnitude

TABLE VI

COMPARISON OF ACTUAL GAS VOLUMES COLLECTED TO THE THEORETICAL VALUES BASED ON THE NUMBER OF COULOMBS PASSED

Date	Run Number	Theoretical Volume O_2(ml)	a:O_2 actual/ O_2 theoretical	Theoretical Volume H_2(ml)	b:H_2 actual/ H_2 theoretical	a/b
8/6/81	1	26.03	0.9074	52.14	0.9852	0.9210
	2	26.03	0.9558	52.15	0.9962	0.9595
	3	26.28	0.9551	52.65	1.0023	0.9529
	4	26.34	0.9556	52.77	0.9991	0.9565
8/17/81	1	27.28	0.8739	54.66	0.9532	0.9168
	2	27.19	0.9559	54.48	0.9945	0.9612
	3	26.73	0.9600	53.56	0.9966	0.9632
	4	26.50	0.9657	53.09	0.9979	0.9677
8/24/81	1 of series 1	23.89	0.9435	47.85	0.9597	0.9831
	2 of series 1	23.93	0.9515	47.93	0.9545	0.9969
	3 of series 1	23.96	0.9482	47.99	0.9560	0.9919
	4 of series 1	23.93	0.9493	47.93	0.9535	0.9949
8/24/81	1 of series 2	23.66	0.9527	47.39	0.9576	0.9949
	2 of series 2	23.84	0.9459	47.76	0.9514	0.9942
	3 of series 2	23.85	0.9430	47.79	0.9473	0.9955
8/25/81	1 of series 1	24.00	0.9033	48.09	0.9798	0.9219
	2 of series 1	24.19	0.9413	48.45	0.9486	0.9923
	3 of series 1	24.23	0.9476	48.54	0.9557	0.9915
	4 of series 1	24.30	0.9436	48.68	0.9552	0.9879
8/25/81	1 of series 2	24.21	0.9527	48.51	0.9534	0.9878
	2 of series 2	24.16	0.9441	48.40	0.9521	0.9917
	3 of series 2	24.24	0.9439	48.56	0.9565	0.9868
	4 of series 2	24.27	0.9423	48.62	0.9525	0.9893
8/26/81	1	24.30	0.9527	48.69	0.9675	0.9846
	2	24.50	0.9633	49.07	0.9633	0.9999
	3	24.54	0.9535	49.16	0.9595	0.9938
	4	24.32	0.9519	48.73	0.9618	0.9897

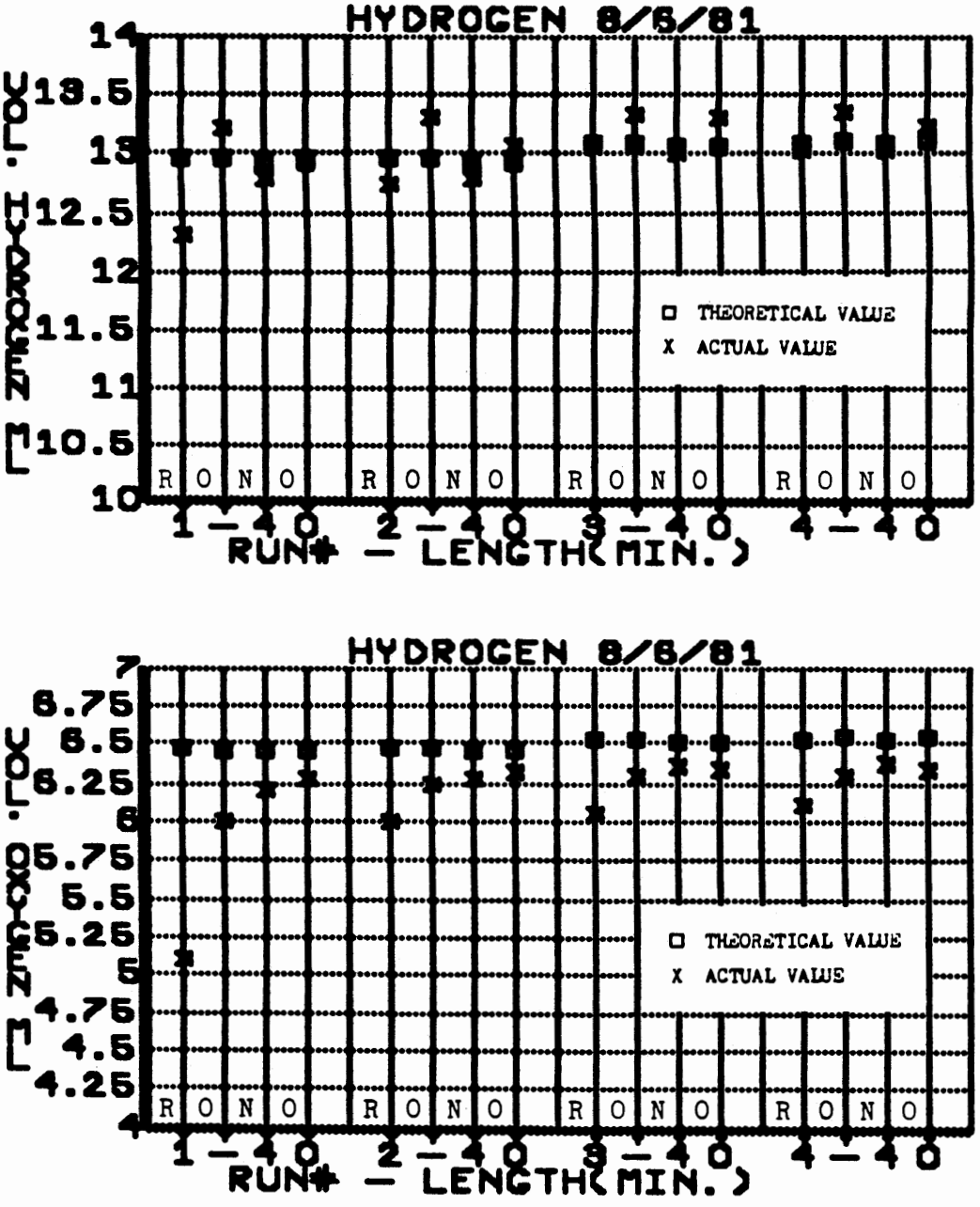

Figure 6. 8/6/81, volume of hydrogen and oxygen collected as a function of the applied magnetic field, with the hydrogen electrode located between the pole pieces. The total length of each run was 40 minutes and each individual segment was 10 minutes long. In the above graphs: R=reverse magnetic field, N=normal magnetic field and 0=magnetic field 'off'. With the magnet current turned on, the applied magnetic field was 1.10 tesla, compared to 0.0150 tesla with the magnet current turned off (i.e. magnetic field off). The electrolyte was 1.81 N H_2SO_4. The applied cell voltage was 8.9916 volts +/- 0.0013 volts.

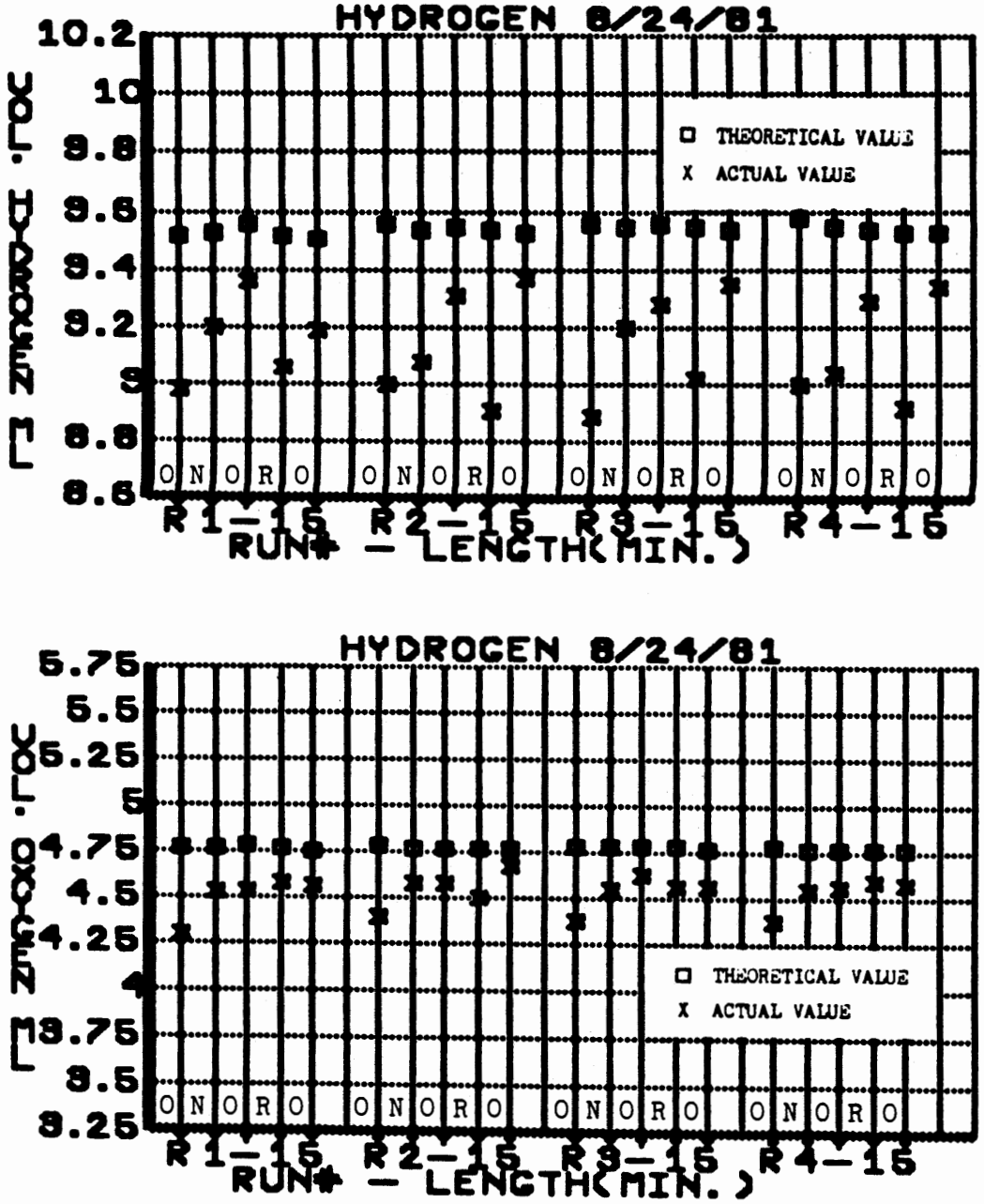

Figure 7. 8/24/81, series 1, volume of hydrogen and oxygen collected as a function of the applied magnetic field, with the hydrogen electrode located between the pole pieces. The total length of each run was 15 minutes and each individual segment was 3 minutes long. In the above graphs: R=reverse magnetic field, N=normal magnetic field and O=magnetic field 'off'. With the magnet current turned on, the applied magnetic field was 1.10 tesla, compared to 0.0150 tesla with the magnet current turned off (i.e. magnetic field off). The electrolyte was 6.34 N H_2SO_4. The applied cell voltage was 9.0263 volts +/- 0.0009 volts.

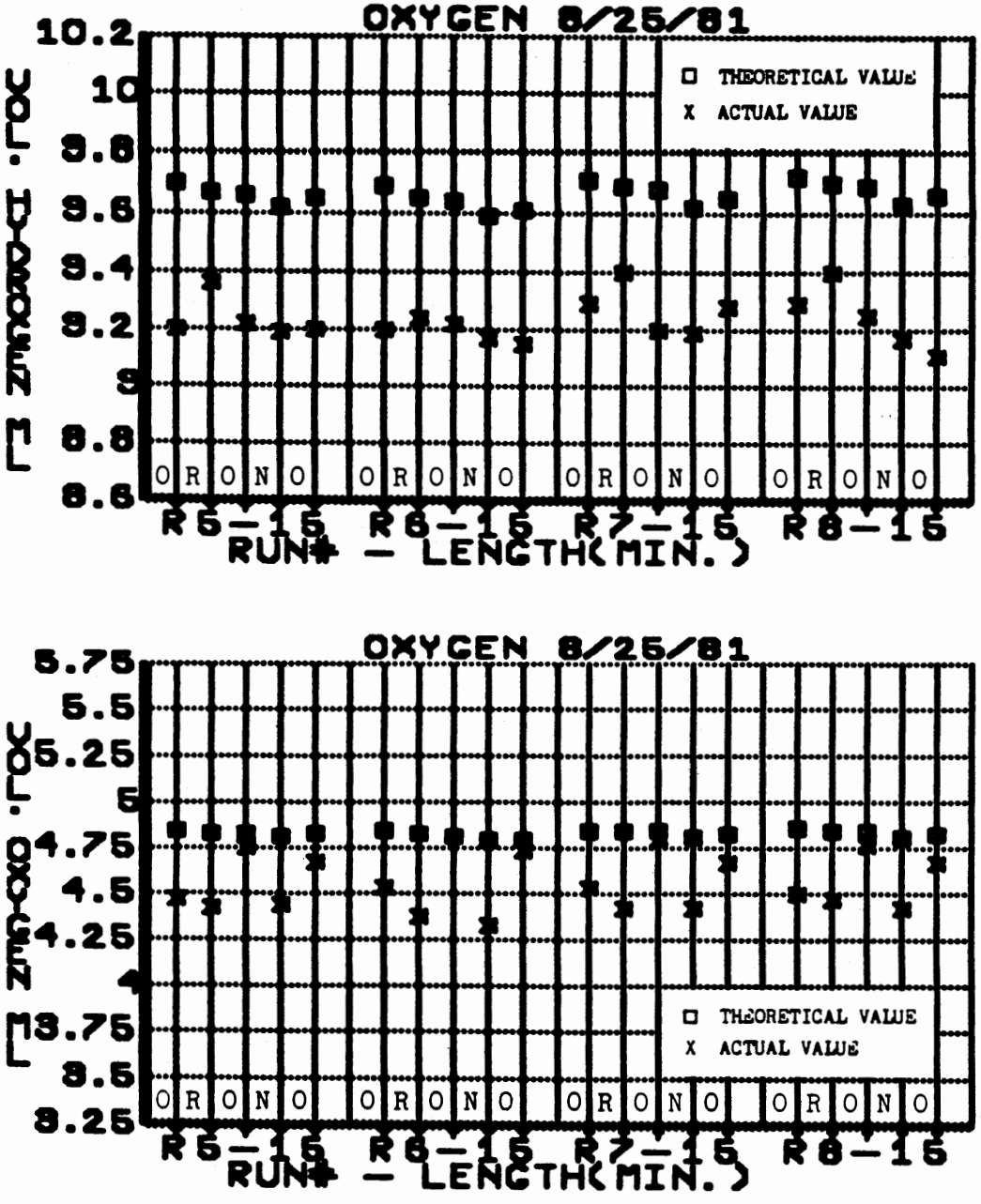

Figure 8. 8/25/81, series 2, volume of hydrogen and oxygen collected as a function of the applied magnetic field, with the oxygen electrode located between the pole pieces. The total length of each run was 15 minutes and each individual segment was 3 minutes long. In the above graphs: R=reverse magnetic field, N=normal magnetic field and O=magnetic field 'off'. With the magnet current turned on the applied magnetic field was 1.10 tesla, compared to 0.0150 tesla with the magnet current turned off (i.e. magnetic field off). The electrolyte was 9.0311 volts +/- 0.0009 volts.

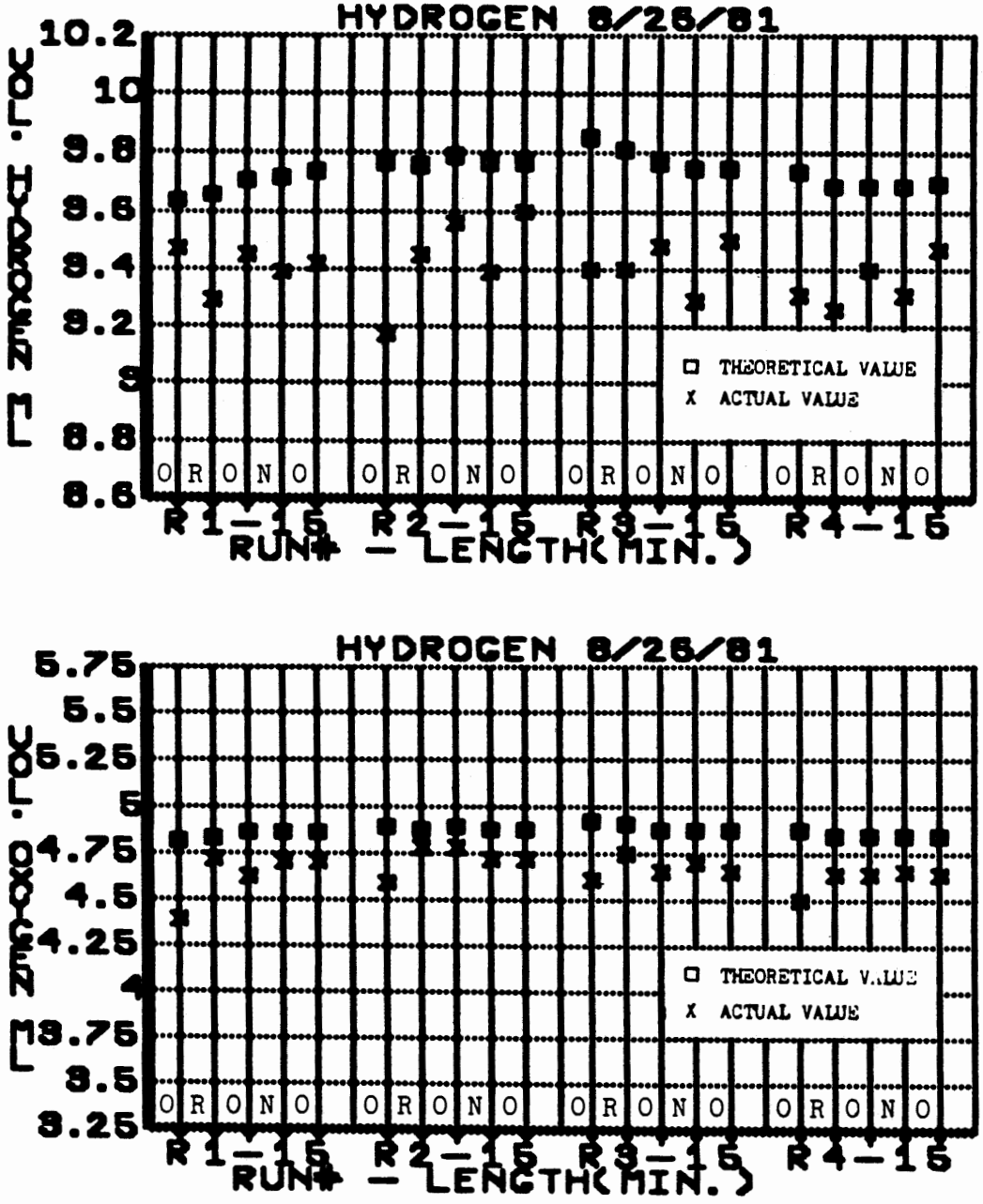

Figure 9. 8/26/81, volume of hydrogen and oxygen collected as a function of the applied magnetic field, with the hydrogen electrode located between the pole pieces. The total length of each run was 15 minutes and each individual segment was 3 minutes long. In the above graphs: R=reverse magnetic field, N=normal magnetic field and O=magnetic field 'off'. With the magnet current turned on, the applied magnetic field was 1.10 tesla, compared to 0.0150 tesla with the magnet current turned off (i.e. magentic field off). The electrolyte was 6.34 N H_2SO_4. The applied cell voltage was 9.0291 volts +/- 0.0021 volts.

of the error produced in the gas volumes is increasing continuously. Figure 10 demonstrates the size of this effect on the hydrogen side of the cell in terms of the total gas volume collected. For example, assume that a total gas volume of 75 ml of gas was collected. Approximately 50 ml of this would be collected on the H_2 side and 25 mlwould be collected on the O_2 side of the cell. From Figure 10 we see that the volume read on the H_2 side of the cell is approximately 0.12 ml low while the O_2 reading is low by approximately one half that amount or 0.06 ml.

Note that Figure 10 is based on a solution containing 50 ml H_2SO_4/liter. For an electrolytic solution containing 175 ml H_2SO_4 /liter the effect would be greater by approximately 12%.

Conclusions

Based on the a/b ratios provided in Table VI, for the runs conducted on 8/24/81 and 8/25/81, it is apparent that the magnetic field has very little effect on the relative total amounts of H_2 and O_2 collected. This is demonstrated by neglecting the first run of each of these days and determining the mean value for the remaining runs; the results of which are given in the following paragraph.

For 8/24/81 the mean a/b value is 0.9947 ± 0.0017 S.D.(n-1) and similarly for 8/25/81 the mean value is 0.9896 ± 0.0022 S.D.(n-1). The difference between these two mean values is approximately 1/2 of 1% and considering the standard deviation values the significance of this difference is questionable.

However, upon examining Figures 7 and 8, it is noted that there

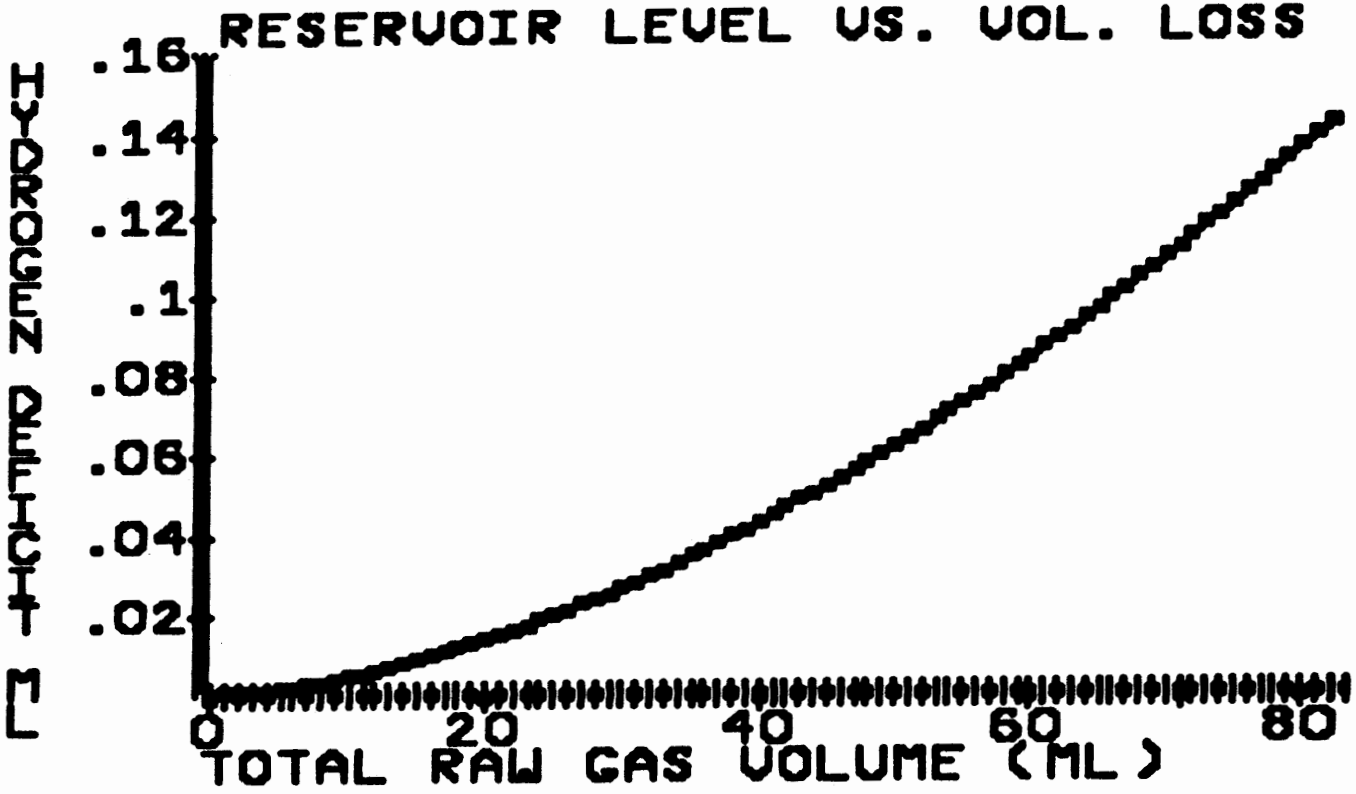

Figure 10. Deficit in the observed gas volume on the hydrogen side of the cell as a function of the total gas volume collected. This figure is actually a computerized simulation of the effect of increasing fluid level in the central reservoir on the total gas volume observed on the hydrogen side of the cell.

was a significant decrease in the volume of gas collected on that side of the cell situated between the pole pieces whenever the magnet current was turned on. For example, for the runs conducted on 8/24/81 with the H_2 electrode located between the pole pieces, it was noted that for runs 1 through 4 the average volume of H_2 collected was 0.33 ml ± 0.10 ml S.D. lower during the intervals with the reverse magnetic field applied compared to the neighboring segments with the magnet current turned off. This number was obtained from the corrected (actual) gas volumes.

The average volume change was obtained by comparing the gas volumes collected in the intervals of interest to the volumes collected during the intervals immediately prior to and following those intervals. From these individual values, the average decrease in the collected gas volume was calculated for the four runs. The corresponding decrease observed on the O_2 side of the cell for the same series of runs (i.e. those shown in Figure 7) was 0.03 ml ± 0.07 ml S.D.

The corresponding values for the other runs are provided in Table VII.

TABLE VII

VARIATIONS IN GAS VOLUMES COLLECTED ASSOCIATED WITH VARIOUS APPLIED MAGNETIC FIELD ORIENTATIONS

Date	Series	ml H_2SO_4 per liter	Electrode between Pole Pieces	Magnetic Field Setting	Change in volume of O_2 collected (ml)	Change in Volume of H_2 collected (ml)
8/6/81	1	50	H_2	Normal	+0.04±0.03 S.D	-0.31±0.05 S.D.
8/17/81	1	50	H_2	Off	+0.04±0.17 S.D.	+0.35±0.13 S.D.
8/24/81	1	175	H_2	Reverse	-0.03±0.07 S.D.	-0.33±0.01 S.D.
8/24/81	2	175	H_2	Normal	-0.05±0.16 S.D.	ex. Run #4
8/25/81	1	175	O_2	Reverse	-0.38±0.11 S.D.	+0.02±0.06 S.D.
8/25/81	2	175	O_2	Normal	-0.34±0.07 S.D.	-0.03±0.02 S.D.
8/26/81	1	175	H_2	Normal	+0.02±0.03 S.D.	-0.14±0.07 S.D.

In the above Table, run #4 of 8/25/81 was deleted from the average for the H_2 side because it was grossly inconsistent with all of the other runs conducted on that day. The same holds true for the entire 2nd series of runs conducted on 8/24/81.

From Table VII, it appears that there was generally a decrease in the amount of gas collected on that side of the cell whose corresponding electrode was located between the pole pieces, during those intervals in which the magnet current was turned on. In five of the six series for which this associated change is given in Table VII, the mean volume change ranges from 0.31 to 0.38 ml.

Based on this fact, it appears that the magnitude of the effect is essentially independent of the orientation of the applied magnetic field, the length of each individual run segment, the electrode exposed

to the applied magnetic field, and the rate at which the gas is being produced.

In the above analysis, it should be noted that just the last three segments of each run were considered, and the volume change was calculated for the middle segment.

Based on the preceding, in conjunction with the a/b ratios given in Table VI, what appears to be the most reasonable conclusion is that there is an increase in the solubility of each of the gases associated with the application of the magnetic field to its corresponding electrode.

Another possible explanation, for this observed behavior, could be that the stirring associated with the magnetic field increases the distance which the bubbles must travel from the electrode to the gas-liquid interface in the gas collecting tube. There is one problem with this explanation which is that during the runs of 8/6/81 and 8/17/81 the rate of gas production was roughly 25 to 30% of that employed during the runs of 8/24/81 to 8/26/81.

EFFECTS ON CELL TEMPERATURE

In this section, a brief discussion of two basic types of temperature changes associated with applied magnetic fields is presented.

The first of these was observed with just one of the electrodes located between the pole pieces. In this case, when the magnet current was turned on or off a noticeable change in the cell temperature was observed approximately 1 cm above the top of the exposed electrode. An accompanying change was also observed at the same elevation above the

opposing electrode in several cases. In both cases the observed temperature change was generally in the range of a few tenths of a degree Celsius or less.

What is interesting about this effect is the fact that quite a bit of variation was observed in the overall magnitude of the effect along with some variation in direction on the anode side of the cell. What was most commonly observed, however, with the anode between the pole pieces, was a decrease in cell temperature when the external magnetic field was applied and an increase in cell temperature when the magnet current was turned off. With the cathode located between the pole pieces, just the opposite effect was observed.

One point worth noting is the fact that, while the change observed on the cathode side was generally smaller in magnitude, the direction of this change was more consistent with the pattern stated above.

The second temperature effect was also observed with just one of the electrodes between the pole pieces. However, in this case, the distance from the point where the temperature was measured to the location of the electrode was approximately 16 cm. For this effect, the orientation of the $\vec{B}$ field was important.

This second effect is apparently closely related to the effect discussed in references (7, 8, 9, 10). This effect will be dealt with in more detail following a brief discussion of the first effect.

Temperature Measured Above Individual Electrodes

This section is based primarily on Figures 11 and 12. Basically,

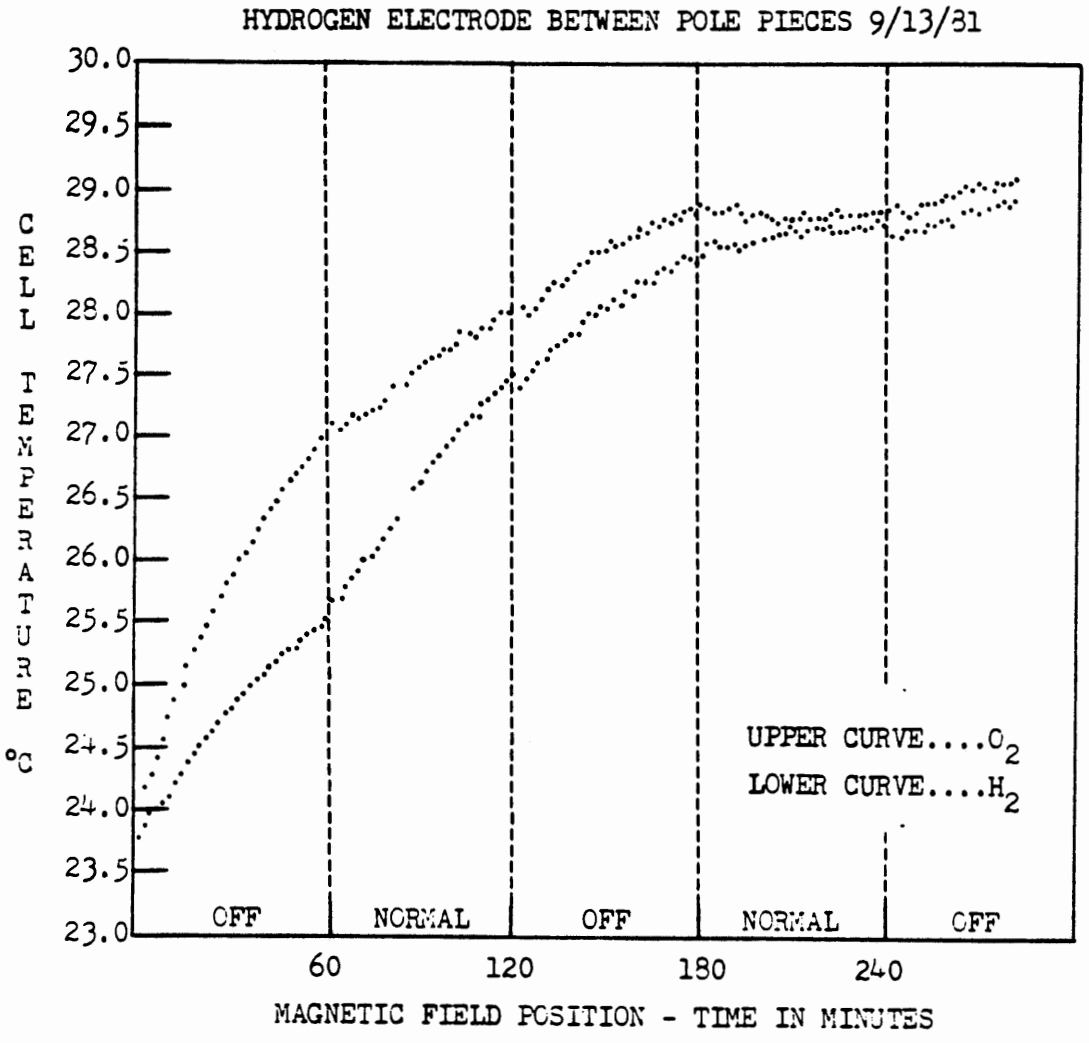

Figure 11. 9/13/81, cell temperature as a function of the applied magnetic field. The temperature was measured about 1 cm above the top of each electrode with the higher temperature being associated with the oxygen electrode. The total length of the run was 280 minutes with the magnetic field being changed at the times shown to the indicated magnetic field orientations. With the magnet current turned on, the applied magnetic field was 1.21 tesla, compared to 0.0155 tesla with the magnet current turned off (i.e. magnetic field off). The electrolyte was 6.34 N H_2SO_4 and the cell current was held constant at 0.24901 amperes +/- 0.00006 amperes.

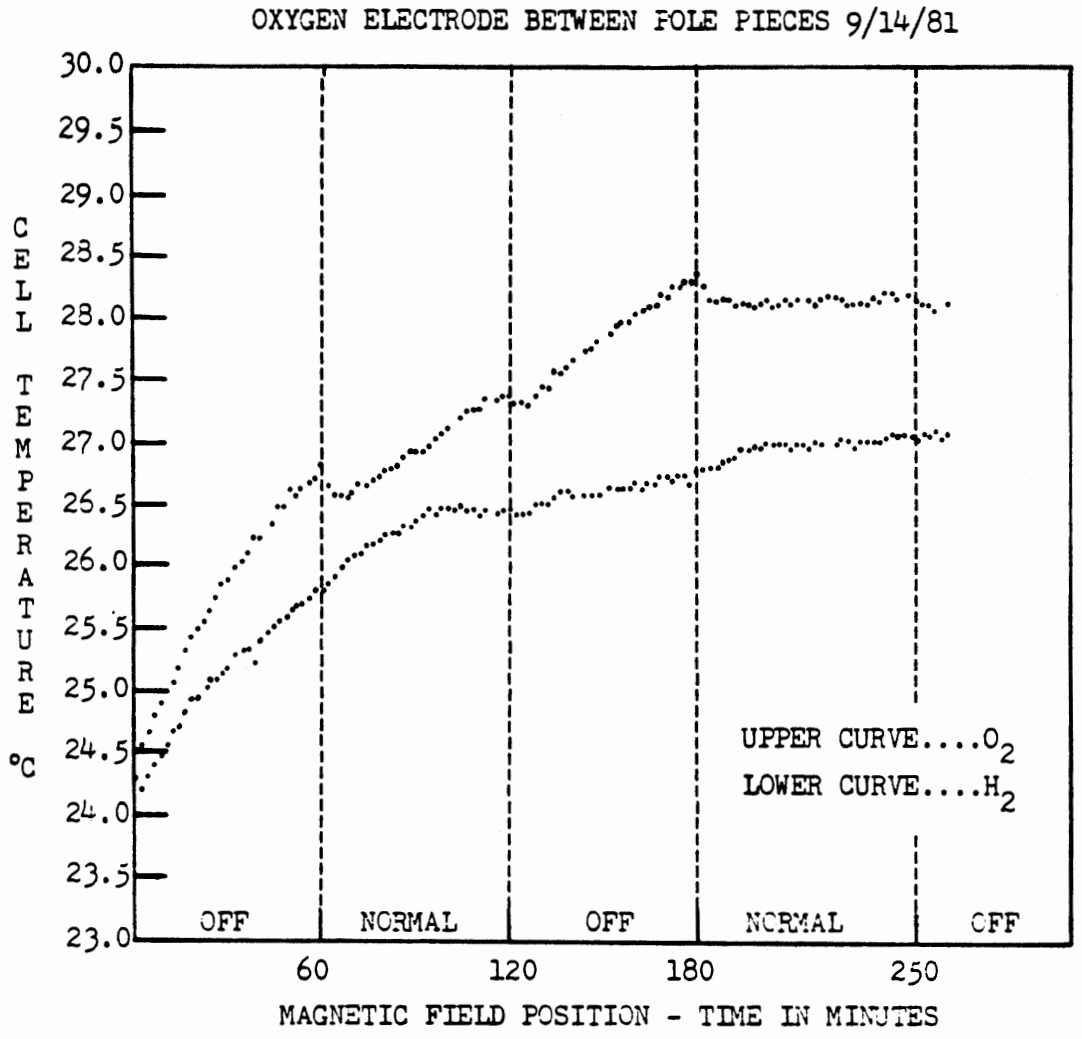

Figure 12. 9/14/81, cell temperature as a function of the applied magnetic field. The temperature was measured about 1 cm above the top of each electrode with the higher temperature being associated with the oxygen electrode. The total length of the run was 260 minutes with the magnetic field being changed at the times shown to the indicated magnetic field orientations. With the magnet current turned on, the applied magnetic field was 1.21 tesla, compared to 0.0155 tesla with the magnet current turned off (i.e. magnetic field off). The electrolyte was 6.34 N H_2SO_4 and the cell current was held constant at 0.25018 amperes +/- 0.00032 amperes.

what is presented in these two figures are the changes in temperature, observed above each electrode when the magnetic field was altered. Based on these and observations from earlier but related runs (for example, see Figure 13), a possible explanation is presented in a qualitative fashion.

The cell that was used to collect the data shown in Figures 11 and 12 is the bottom half of the cell shown in Figure 4. (e.g. The central reservoir and the gas collecting tubes have been removed.) Once again the cell was thermally insulated; however, as an additional precaution, the cooling water for the electromagnet was manually regulated to maintain a more constant cooling jacket temperature.

Due to polarization, there is excess joule heating near the anode and the cathode; however, the power output at the anode is about 4.5 times that encountered near the cathode (for a current density of 0.1 amp/cm^2)(15). The above offers a possible explanation for the fact that temperature readings taken near the oxygen electrode were consistently higher than those obtained near the hydrogen electrode.

This may also explain the variations in cell temperature associated with the application and removal of the $\vec{B}$ field. For example, if the thermal conductivity of the electrolyte, near the electrode, is equal to some value K prior to turning on the magnet current, then one should expect this value to increase to a value K' following the application of the $\vec{B}$ field. (An increase is expected due to stirring associated with the $\vec{B}$ field.)

The above, in conjunction with the fact that the exposed volume was essentially the same no matter which electrode was between the pole

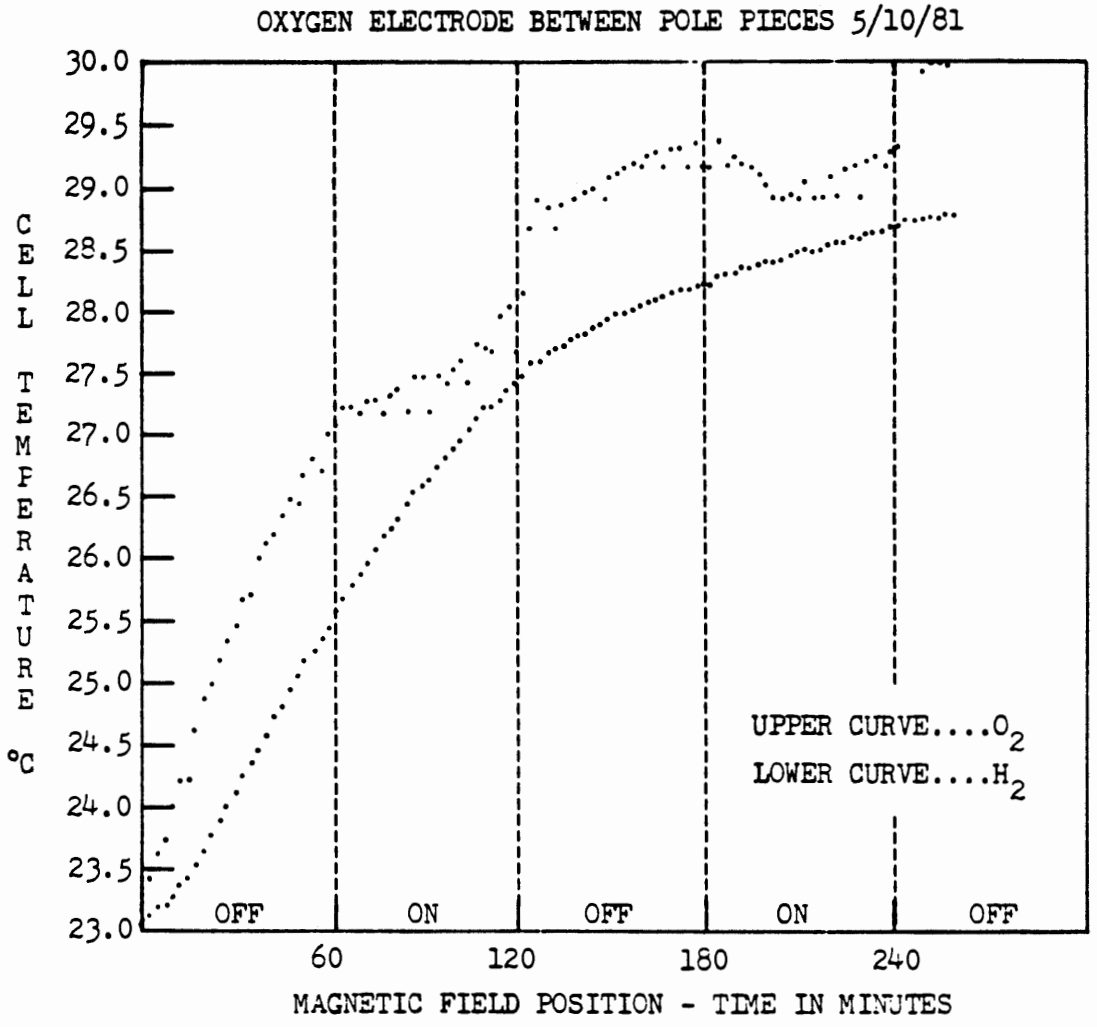

Figure 13. 5/10/81, cell temperature as a function of the applied magnetic field. The temperature was measured about 1 cm above the top of each electrode with the higher temperature being associated with the oxygen electrode. The total length of the run was 260 minutes with the magnetic field being changed at the times shown to the indicated magnetic field orientations. With the keepers removed the permanent magnet produced a magnetic field of 0.1750 tesla, compared to 0.0150 tesla with the keepers on (i.e. magnetic field off). The electrolyte was 1.81 N H_2SO_4 and the cell current was held constant at 0.14990 amperes +/- 0.00005 amperes.

pieces, should lead one to expect some basic differences between the temperature effects observed above the anode and the cathode when exposed to the $\vec{B}$ field on an individual basis.

During the experimental work represented in Figures 10 and 11 the applied $\vec{B}$ field was 1.21 tesla with the magnet current turned on and 0.0150 tesla with the current turned off.

Temperature Measured Between Electrodes

The second temperature effect, associated with changes in the magnetic field, was observed in the central portion of the cell and appears to be related to the effect discussed in references (7, 8, 9, 10). The characteristics of the effect were given in Chapter I based primarily on the work of E. Tronel-Peyroz, et al. (7).

The experimental cell is shown in Figure 4. The temperature readings shown in Figures 14-18 were recorded for the same runs discussed earlier in the gas collection portion of this chapter. All of the temperature readings were taken in the central vertical tube approximately 1 cm above the top of the main cross tube.

On the following pages, a breakdown of the results obtained for 8/24/81, H_2 electrode between the pole pieces and for 8/25/81, O_2 electrode between the pole pieces is presented. In these two cases, a 6.34 normal solution of H_2SO_4 was used.

Along with the above breakdown, there is included a brief discussion of earlier results obtained with a 1.81 normal solution (see Figure 14).

In this section an attempt is made to compare our experimental

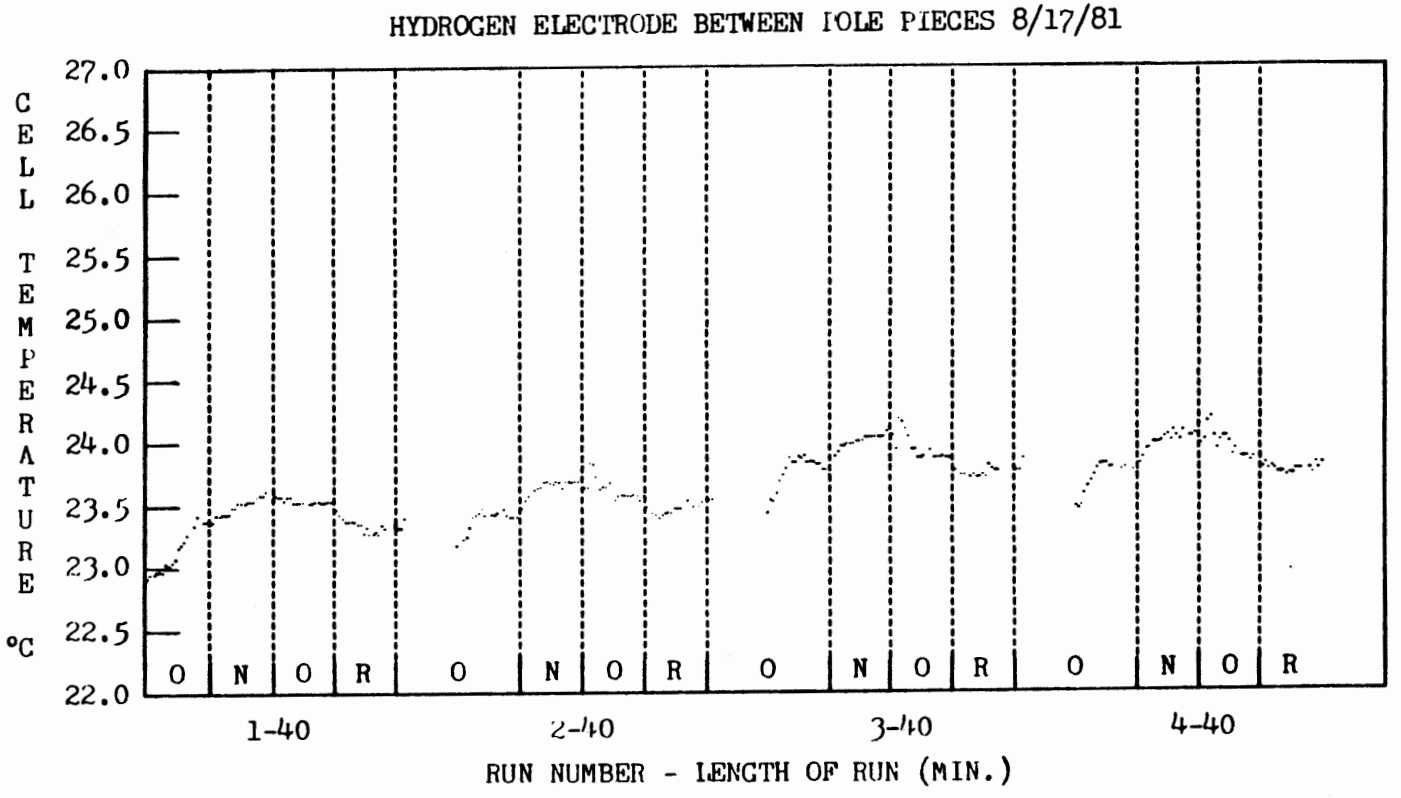

Figure 14. 8/17/81, cell temperature as a function of the applied magnetic field. The total length of each run was a minimum of 40 minutes, and each individual segment was 10 minutes long. The temperature was measured in the center vertical tube about 1 cm above the top of the main cross tube. In the above graph: R = reverse magnetic field, N = normal magnetic field and O = magnetic field 'off'. With the magnet current turned on, the applied magnetic field was 1.10 tesla, compared to 0.0150 tesla with the magnet current turned off (i.e. magnetic field off). The electrolyte was 1.81 N H_2SO_4. The applied voltage was 8.9805 volts +/- 0.0030 volts.

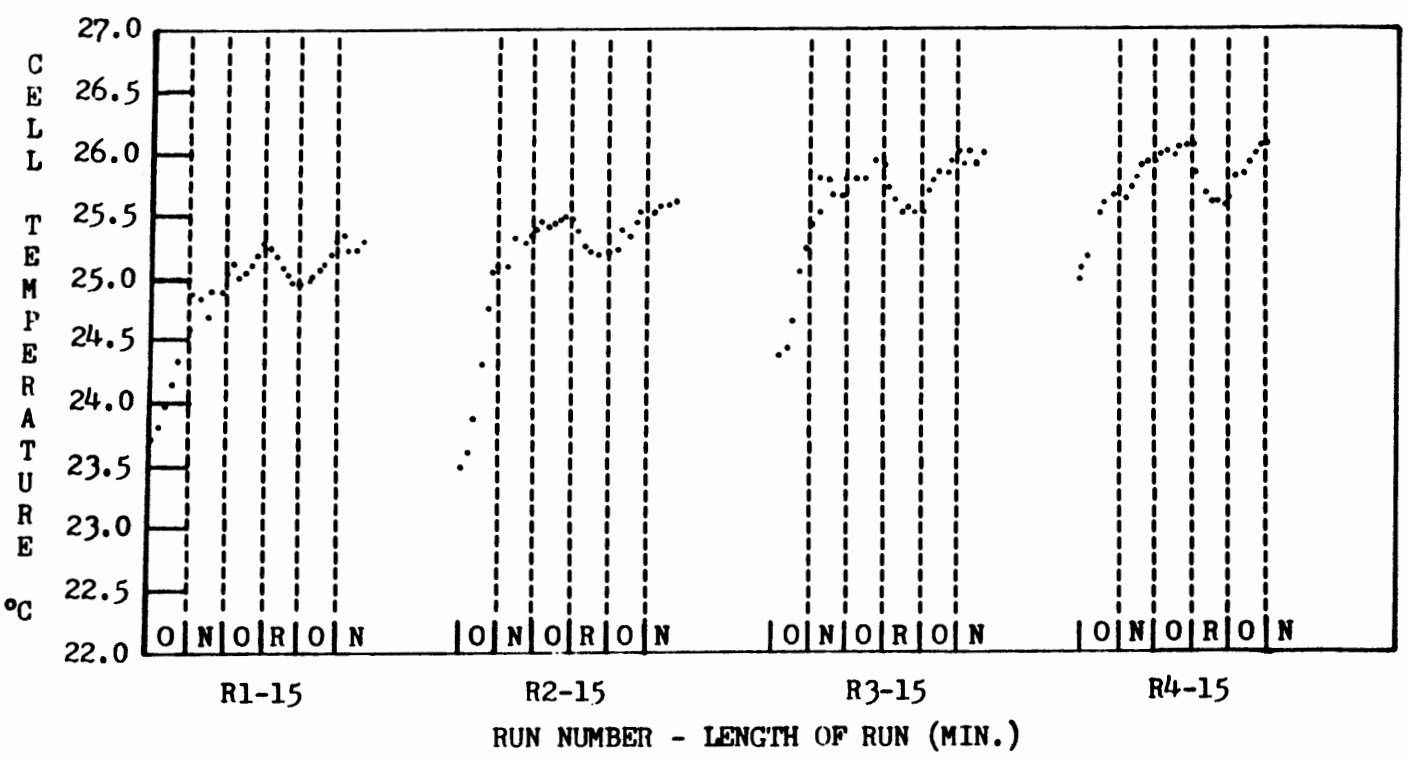

Figure 15. 8/24/81, series 1, cell temperature as a function of the applied magnetic field. The total length of each run was a minimun of 15 minutes and each individual segment was 3 minutes long. The temperature was measured in the center vertical tube about 1 cm above the top of the main cross tube. In the above graph: R = reverse magnetic field, N = normal magnetic field and 0 = magnetic field 'off'. With the magnet current turned on, the applied magnetic field was 1.10 tesla, compared to 0.0150 tesla with the magnet current turned off (magnetic field off). The electrolyte was 6.34 N H_2SO_4. The applied voltage was 9.0263 volts +/- 0.0009 volts.

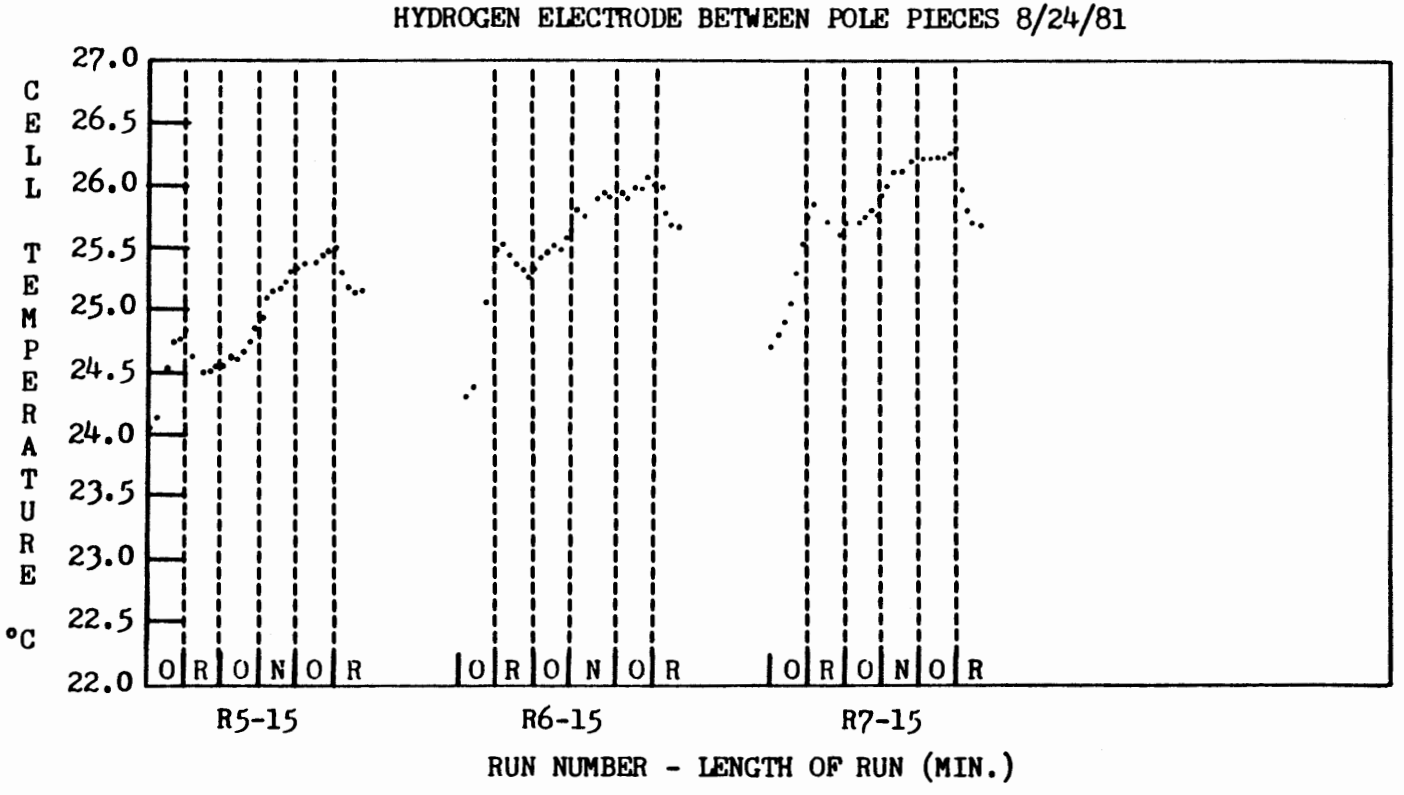

Figure 16. 8/24/81, series 2, cell temperature as a function of the applied magnetic field. The total length of each run was a minimum of 15 minutes and each individual segment was 3 minutes long. The temperature was measured in the center vertical tube about 1 cm above the top of the main cross tube. In the above graph: R = reverse magnetic field, N = normal magnetic field and 0 = magnetic field 'off'. With the magnet current turned on, the applied magnetic field was 1.10 tesla, compared to 0.0150 tesla with the magnet current turned off (magnetic field off). The electrolyte was 6.34 N H_2SO_4. The applied voltage was 9.0296 volts +/- 0.0017 volts.

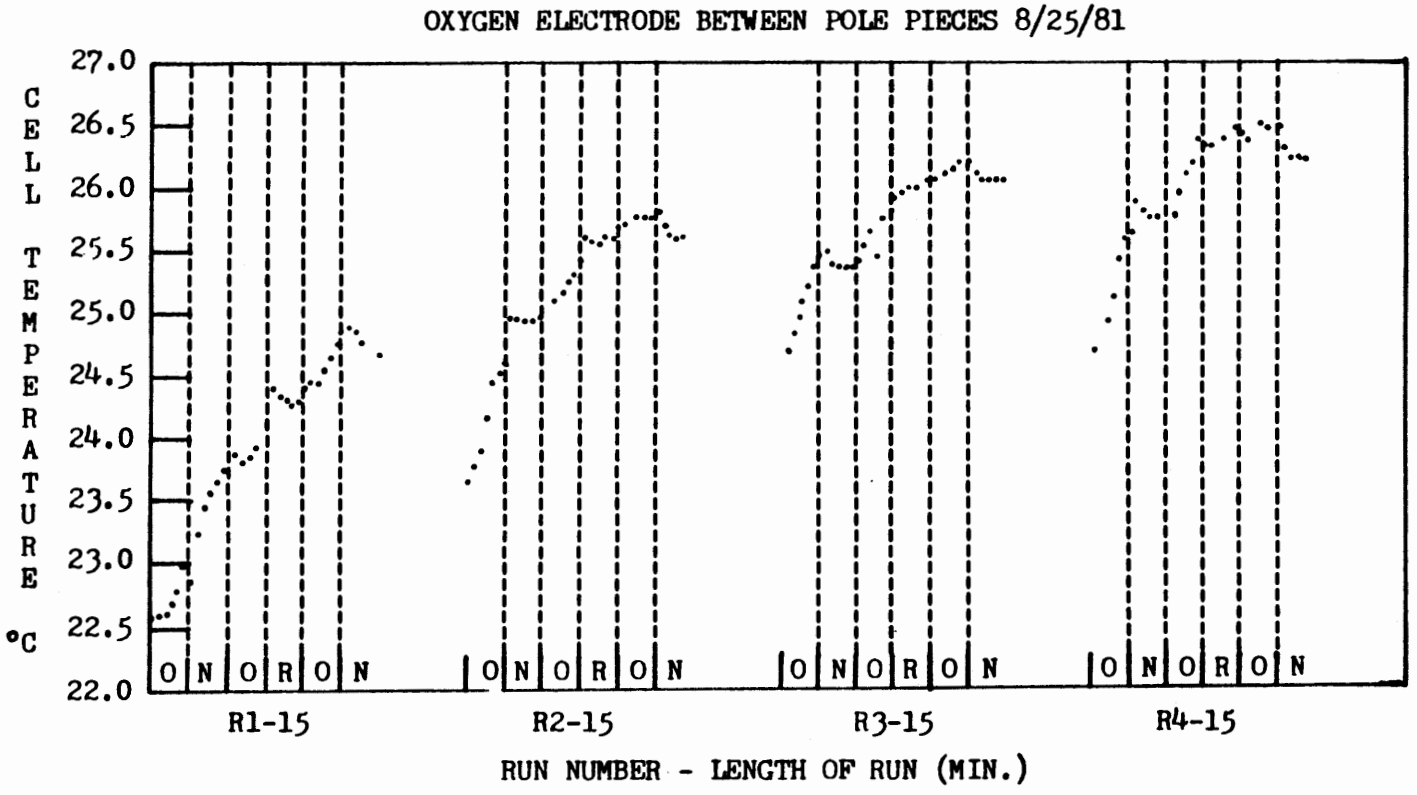

Figure 17. 8/25/81, series 1, cell temperature as a function of the applied magnetic field. The total length of each run was a minimum of 15 minutes and each individual segment 3 minutes long. The temperature was measured in the center vertical tube about 1 cm above the top of the main cross tube. In the above graph: R = reverse magnetic field, N = normal magnetic field and 0 = magnetic field 'off'. With the magnet current turned on, the applied magnetic field was 1.10 tesla, compared to 0.0150 tesla with the magnet current turned off (magnetic field off). The electrolyte was 6.34 N H_2SO_4. The applied voltage was 9.0325 volts +/- 0.0021 volts.

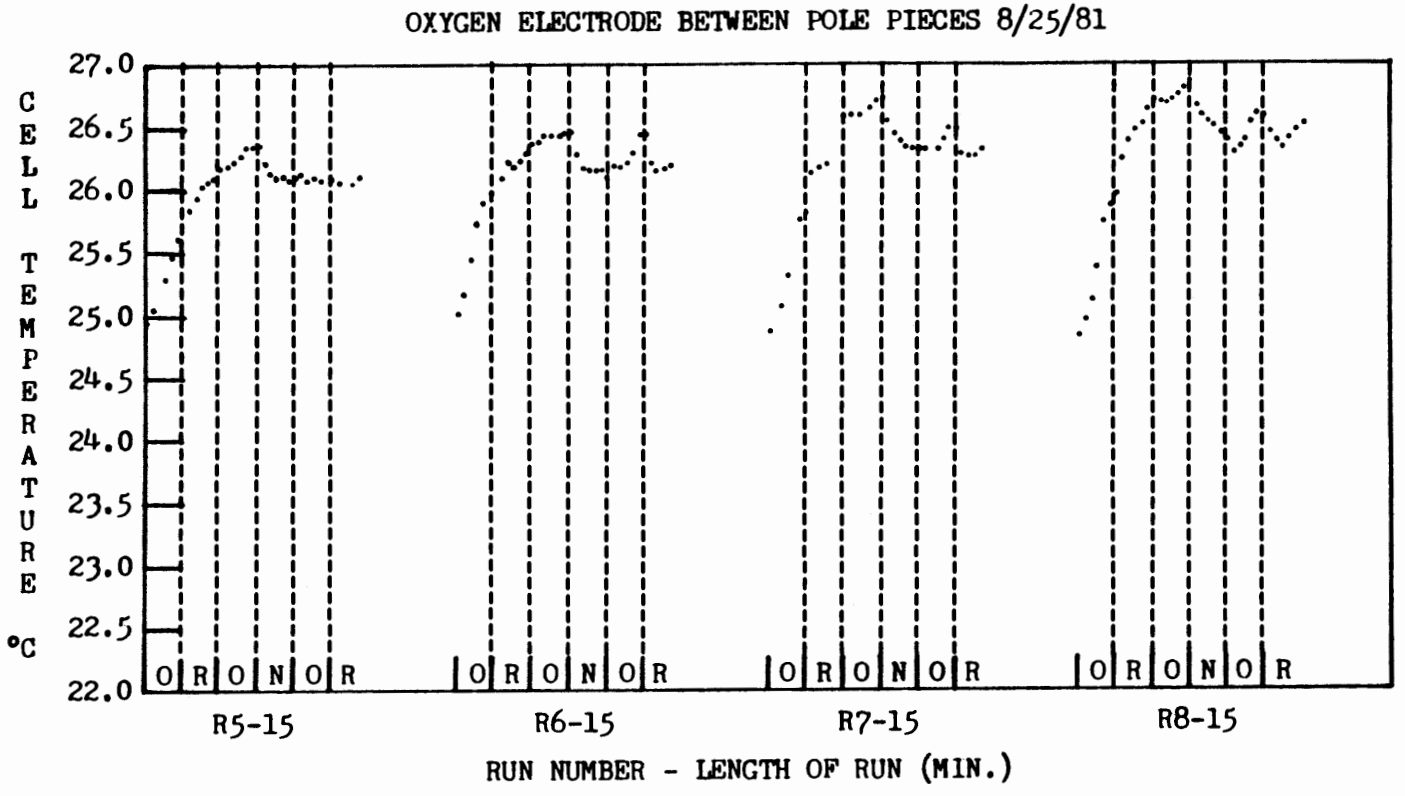

Figure 18. 8/25/81, series 2, cell temperature as a function of the applied magnetic field. The total length of each run was a minimum of 15 minutes and each individual segment was 3 minutes long. The temperature was measured in the center vertical tube about 1 cm above the top of the main cross tube. In the above graph: R = reverse magnetic field, N = normal magnetic field and O = magnetic field 'off'. With the magnet current turned on, the applied magnetic field was 1.10 tesla, compared to 0.0150 tesla with the magnet current turned off (magnetic field off). The electrolyte was 6.34 N H_2SO_4. The applied voltage was 9.0311 volts +/- 0.0009 volts.

results to related data presented in graphical form in reference (7). Their graph was also obtained experimentally; however, the setup used to collect their data differs from ours in several important aspects, including the following:

a) In reference (7), the electrolyte was a mixture of HCL and H_2O, with the normality ranging between 0.025 N and 0.5 N.

b) Also in reference (7), several different cells were used as described in Chapter I. The widest cell was 4 mm compared to the inner diameter of 17.4 mm for the main cross tube in our experiment.

c) Another important difference is that, in reference (7) the electrodes were placed outside the magnetic field, while the temperature variations were recorded within a uniform $\vec{B}$ field of 0.5 tesla. The $\vec{B}$ field in our experiment varied as shown in Figure 2 with the $\vec{B}$ field falling off to about 0.055 tesla at the position where the temperature change was measured (approximately 14.5 to 15 cm away from the center of the region enclosed by the pole pieces.)

Examining the temperature readings associated with the runs of 8/24/81 (Figures 15 and 16, H_2 electrode between the pole pieces) and the runs of 8/25/81 (Figures 17 and 18, O_2 electrode between the pole pieces) the following observations were made:

a) For the runs of 8/24/81, turning on the normal mangetic field produced very little effect on the measured temperature. However, turning on the reverse magnetic field decreased the cell temperature by 0.25 to 0.50°C in the brief time span allowed (3 minutes).
This pattern held true even when the relative positions of normal and reverse applied magnetic field intervals were interchanged.

b) Contrasting with the above, and although somewhat less clear cut, for the runs of 8/25/81 it appears that the normal magnetic field was much more effective at decreasing the measured cell temperature than was the reverse magnetic field of the same magnitude. The observed decreases in cell temperature were generally comparable in magnitude to those noted in part (a).

From previous runs with the H_2 electrode located between the pole

pieces for which the same cell was used, but with only 50 ml H_2SO_4 /liter and a lower cell current, it was observed that turning the magnetic field from the 'off' position to the normal position forces the measured temperature to increase by approximately 0.2°C ± 0.05°C (see Figure 14 for example). And, as would be expected based on the results outlined for 8/24/81, when the reverse magnetic field was applied a decrease in the cell temperature of approximately 0.15°C ± 0.05°C was observed.

During the 40 minute runs, the cell current varied from a minimum value of 167 ma to a maximum of 181 ma yielding an overall average of 174 ma.

Similarly, for the 15 minute runs the minimum cell current was 412 ma and the maximum cell current was 432 ma for an average value of 422 ma.

In summary, it should be stressed that for the 15 minute runs of 8/24/81 and 8/25/81 while cooling did occur near the top of the main cross tube with the Lorentz force directed downward, heating was not detected when the Lorentz force was directed upward. Normally, during the primary portion of the run, there was very little if any change observed when an increase was expected (7) in conjunction with the applied magnetic field.

During the 40 minute runs, with the Lorentz force directed downward, cooling was also detected. The observed change being about 1/3 to 1/2 that observed in the 15 minute runs. However, when the Lorentz force was directed upward an increase of up to 0.25°C was observed as expected (7) (in contrast to the 15 minute runs).

Table VIII was obtained from the graph (7) described previously. The temperatures of the electrolyte solutions included in this table were between 18.3°C and 20.3°C.

The general experimental setup is described in Chapter I under the subtitle 'Thermomagnetoelectric Effects'.

TABLE VIII

CELL CURRENT REQUIRED FOR ΔT_s^{∞} TO EQUAL 0.25°C AS A FUNCTION OF NORMALITY AND CELL WIDTH

Normality HCL	Z dimension in mm	ΔT_s^{∞} (°C)	Cell Current in milliamps
0.025	2	0.25	12.1 ± 0.2
0.05	1	0.25	19.7 ± 0.2
0.05	2	0.25	21.9 ± 0.2
0.1	2	0.25	30.1 ± 0.2
0.1	3	0.25	33.5 ± 0.2
0.1	4	0.25	35.5 ± 0.2
0.5	2	0.25	54.7 ± 0.2

If two graphs are made of the data given in Table VIII, one based on the data provided for 0.1 N HCL and the other based on the data provided for Z = 2 mm, then from the first graph cell current as a function of cell width is obtained and from the second graph one obtains cell current as a function of the normality.

If the first graph is extended to a width of 18 mm, based on the curve set up by the first three points, along with the assumption that the required cell current approaches zero as the cell width (Z dimension) approaches zero, then the ratio of the cell current for Z = 17.4 mm to Z = 2 mm is approximately 40 ma/30 ma = 1.33.

Extending the second graph in a similar manner, the ratio of the

required current for N = 1.81 to N = 0.5 is approximately 98 ma/54.7 ma = 1.79.

Combining the data from these two graphs (and assuming that the product of these two effects provides a valid result), then for a 1.81 normal HCl solution, with a cell 17.4 mm wide, the current required to produce a ΔT_s^{∞} value of 0.25°C should be

(1.33)(98 ma) = 130 ma.

The preceeding is for a uniform $\vec{B}$ field of 0.5 tesla, which is approximately nine times the magnitude of the $\vec{B}$ field where our temperature readings were taken, with the electromagnet turned 'on'. There is a significant difference, however: the $\vec{B}$ field in our experiments was a function of the distance form the center of the region enclosed by the pole pieces as is shown in Figure 3. In conjunction with this, the electrode between the pole pieces was exposed to a $\vec{B}$ field of 1.1 tesla while the other electrode was exposed to a $\vec{B}$ field of approximately 0.002 tesla. Furthermore, it should be noted that a portion of ΔT_s^{∞} appears to be independent of $\vec{B}$ (7, 9, 10).

The data discussed in (7) was for various normalities of HCl while our data was obtained for H_2SO_4 solutions of a much greater normality (roughly 3.6 and 12.7 times the highest normality given in Table VIII).

Considering the differences between the two groups of experiments with respect to temperature, normality, cell thickness, type of acid, and the nature of the applied $\vec{B}$ field it seems rather amazing that the two sets of experiments agree as well as they do.

It appears that the same fundamental temperature change was

observed in both sets of experiments. The observed differences may very well be due to the factors listed in the preceeding paragraph.

CHAPTER IV

EFFECTS OF MAGNETIC FIELDS ON CELL VOLTAGE

In this chapter, a discussion of the voltage changes observed following the application or removal of an applied magnetic field (both with and without pumping the electrolyte through the cell), during the processes of electrolytic deposition and removal of copper is presented and compared to related literature (3, 4, 5).

EXPERIMENTAL SETUP

During these experiments, most of the runs were performed using the cell shown in Figure 17. Some further analysis was completed using the bottom half of the cell shown in Figure 3, (i.e. the gas collecting tubes and central reservoir were removed). The electrolyte was a solution of 0.5 M H_2SO_4 and 0.5 M $CuSO_4$.

The electrodes used for these experiments were made of high purity copper (Anala R copper, not less than 99.9% Cu, product no. 10085, BDH Chemicals Ltd, Poole England). Prior to electrolysis the electrodes were approximately 0.94 cm x 1.27 cm and one of the sides was coated with microstop. The thickness of the electrodes was about 0.120 mm and the entire exposed area was roughly 1.19 cm^2. For these experiments a current density of 800 amp/m^2 was desired, so a cell current of approximately 0.0953 amps $\pm$ 0.0003 amps was used. The uncertainty indicates the maximum spread observed in the cell current for all of

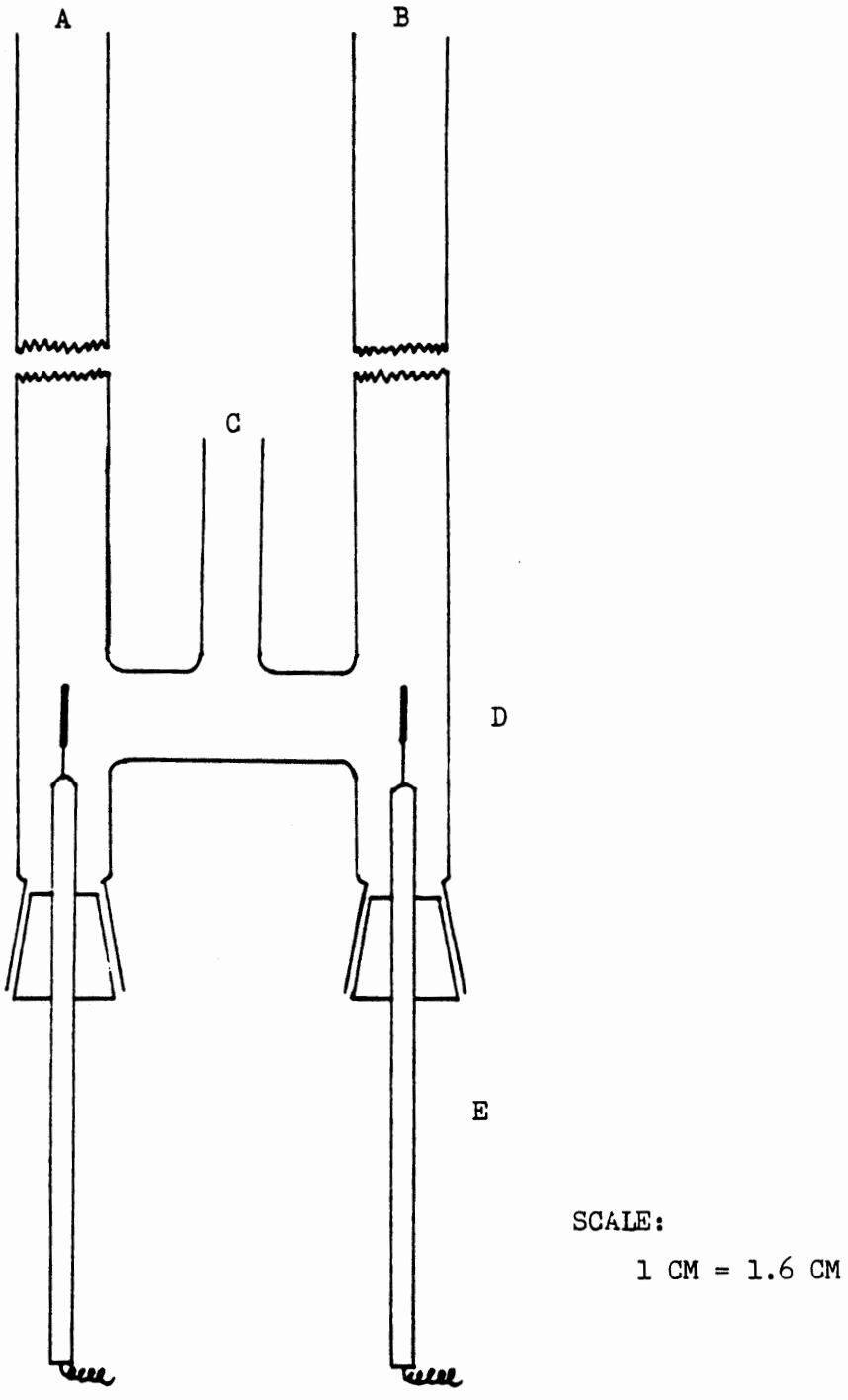

Figure 19. Primary cell used during the electrolysis of copper experiments. A, B and C identify the various inlets into the main body of the glass cell. D is the copper electrode and E is the electrode holder.

the runs utilizing the cell shown in Figure 19. (For any given run, the cell current was generally much more constant than this.)

The actual steps used during the runs conducted with the cell shown in Figure 19 are listed in the next section.

The four-inch pole pieces were used for all of the runs utilizing the cell shown in Figure 19, while the two inch pole pieces were used for the run completed with the bottom half of the cell shown in Figure 4. In both cases, when the magnet current was turned on the $\vec{B}$ field between the pole pieces was equal to 1.15 tesla and when the magnet current was turned off the $\vec{B}$ field decreased to 0.0155 tesla.

The cell shown in Figure 19 was set up in such a manner that it was possible to pump the electrolyte through the cell when desired. It should also be noted that this cell was tilted backwards at 30° from the vertical in order to reduce the problems associated with the elimination of bubbles from the system.

EXPERIMENTAL RESULTS

The experimental results obtained with the cell shown in Figure 19 demonstrated a decrease in the cell voltage each time the magnet current was turned on along with a similar increase in the cell voltage when the magnet current was turned off. This was true whether just the anode or the cathode or both were placed between the pole pieces. However, it was observed that on the average the change in cell voltage was the greatest with just the single cathode located between the pole pieces. This was followed fairly closely by the cathode-anode combination, while the resulting change associated with the single anode was a

distant third.

In Table IX, a break down of the observed changes in the cell voltage is presented. Several runs were completed in each of the three modes with the electrolyte being pumped into the center tube and out both sides when indicated.

For this table, when both electrodes were located between the pole pieces, the electrode listed first is the one which was located nearest the front of the electromagnet. This distinction is not made in the text unless specifically noted.

The basic sequence used for each run was as follows:

1. Start electrolysis process.
2. Start pumping the electrolyte through the cell.
3. Turn off pump.
4. Turn magnet current on, magnetic field normal.
5. Start pumping the electrolyte through the cell.
6. Turn off pump.
7. Turn off magnet current.
8. Turn magnet current on, magnetic field reverse.
9. Start pumping the electrolyte through the cell.
10. Turn off pump.
11. Turn off magnet current.

Normally, whatever change was observed in the cell voltage, following each of the steps in the preceding sequence, normally began immediately and in most cases had maximizied itself and reached some quasi-stable value after 15 seconds, although in some instances the time period required was slightly longer. The average time between each of the steps in the above sequence was between 1 and 2 minutes. The voltage changes given in Table IX were obtained by taking the difference between the starting voltage and the quasi-stable value associated with that step.

The voltage values given in Table IX were obtained from the plot

TABLE IX

OBSERVED CHANGES IN THE CELL VOLTAGE DURING THE ELECTRODEPOSITION OF COPPER UNDER VARIOUS EXPERIMENTAL CONDITIONS

Electrode(s) Between Pole Pieces	(Step No.) Action Applied	Starting Cell Voltage (volts)	Change in Cell Voltage (Volts)	Ratio of Change in Cell Voltage
Cathode and Anode	(2)start pump	2.275	-.280	1.00
Anode and Cathode	(2)start pump	2.420	-.410	1.46
Cathode	(2)start pump	2.355	-.365	1.30
Anode	(2)start pump	2.335	-.330	1.18
Cathode and Anode	(3)stop pump	1.995	+.240	1.00
Anode and Cathode	(3)stop pump	2.015	+.265	1.10
Cathode	(3)stop pump	1.990	+.355	1.48
Anode	(3)stop pump	2.015	+.240	1.00
Cathode and Anode	(4)magnet on normal	2.220	-.200	1.00
Anode and Cathode	(4) " "	2.285	-.215	1.08
Cathode	(4) " "	2.295	-.265	1.33
Anode	(4) " "	2.245	-.020	.10
Cathode and Anode	(5)start pump	2.050	-.030	1.00
Anode and Cathode	(5)start pump	2.070	-.035	1.17
Cathode	(5)start pump	2.035	-.030	1.00
Anode	(5)start pump	2.230	-.195	6.50
Cathode and Anode	(6)stop pump	2.020	+.030	1.00
Anode and Cathode	(6)stop pump	2.035	+.050	1.67
Cathode	(6)stop pump	2.020	+.040	1.33
Anode	(6)stop pump	2.035	+.165	5.50
Cathode and Anode	(7)magnet off	2.050	+.160	1.00
Anode and Cathode	(7)magnet off	2.090	+.155	.97
Cathode	(7)magnet off	2.095	+.245	1.53
Anode	(7)magnet off	2.195	+.020	.13
Cathode and Anode	(8)magnet on reverse	2.190	-.125	1.00
Anode and Cathode	(8) " "	2.240	-.145	1.16
Cathode	(8) " "	2.335	-.215	1.72
Anode	(8) " "	2.205	-.045	.36

TABLE IX (cont.)

Electrode(s) Between Pole Pieces	(Step No.) Action Applied	Starting Cell Voltage (volts)	Change in Cell Voltage (Volts)	Ratio of Change in Cell Voltage
Cathode and Anode	(9)start pump	2.065	-.020	1.00
Anode and Cathode	(9)start pump	2.095	-.050	2.50
Cathode	(9)start pump	2.140	-.040	2.00
Anode	(9)start pump	2.160	-.105	5.25
Cathode and Anode	(10)stop pump	2.045	+.020	1.00
Anode and Cathode	(10)stop pump	2.050	+.045	2.25
Cathode	(10)stop pump	2.110	+.035	1.75
Anode	(10)stop pump	2.070	+.120	6.00
Cathode and Anode	(11)magnet off	2.070	+.115	1.00
Anode and Cathode	(11)magnet off	2.110	+.135	1.17
Cathode	(11)magnet off	2.150	+.190	1.65
Anode	(11)magnet off	2.195	+.040	.35

of the cell voltage produced by the strip chart recorder. This was used in preference to the computer print out, because the analog nature of the plot made it possible to allow for the 'noise' in the system, which was rather large at times. In addition, it was easier to tell when the system had reached its quasi-stable value.

There were no primary effects on the cell voltage resulting from the fact that the cell was tilted backwards. However, it was noted that with the anode in front when the magnet current was turned off and the cell voltage started to climb it would quickly overshoot what was to be the quasi-stable value, peak rapidly and fall back to the quasi-stable value. With the cathode in front this behavior was not observed, instead the voltage would rise to the quasi-stable value without the intermediate peaking step. In both cases the time required to reach the quasi-stable value was roughly the same.

The behavior described above does not seem to depend on whether the anode was between the pole pieces by itself or in conjuction with the cathode. It was also observed with both the normal and reverse $\vec{B}$ field orientations. Furthermore, if the pump was running with the magnetic field turned off when the pump was turned off this same peaking behavior was observed.

Examining the data given in Table IX, the first important point to note is that, just prior to the application of step number 3, all 4 cell voltage values were fairly close.

Then when step number 4 was applied, decreases in the cell voltage were noted in all four cases, with the decrease for the single cathode being the largest and the decrease for the single anode being

the smallest.

The sequence was followed in turn by the application of step number 5 (turning on the pump and pumping 1.7 liters of electrolyte through the cell per minute) which caused an associated decrease in the cell voltage for the single anode which was 5.5 to 6.5 times as large as that associated with any other electrode combination.

When the pump was turned off, followed in turn by the magnetic field, the same qualitative changes were noted but in the opposite direction, as might be expected. Likewise, in a qualitative manner, the same sequence of events occurred when the reverse orientation of the applied magnetic field was used.

To examine the possibility that part of the observed decrease in the cell voltage with the single anode located between the pole pieces, may be due to the interaction of the magnetic field with the cathode, the experiment was repeated utilizing the cell shown in Figure 4. This possibility was examined since the $\vec{B}$ field, at the position of the cathode was approximately 0.13 to 0.14 tesla.

The results of this experiment, likewise, indicated a decrease in the cell voltage when the magnetic field was applied. However, the decrease in cell voltage was roughly three-quarters of that observed previously. (The cathode in this case was exposed to a magnetic field of approximately 0.002 tesla when the magnet current was turned on).

The cell voltage associated with the cell shown in Figure 4 was approximately 7 volts, which is roughly 3 to 3 1/2 times that associated with the cell shown in Figure 19. Once again the constant current mode was utilized with a current density of approximately 800 amps/m^2.

The cell temperature was 24.5°C ± 1°C for most of the data given in Table IX. This temperature was determined from measurements taken with chromel-alumel thermocouples approximately 1 cm above the tops of both the anode and the cathode.

One noteworthy observation concerning these experiments is that the lowering of the cell voltage due to pumping the electrolyte through the cell and the decrease in cell voltage due to the magnetic field are not independent of each other. This was shown in earlier runs for which very little (e.g. 0.005 volts or less) or no change in the cell voltage was observed when the magnet current was turned on or off in both the normal and reverse modes while the electrolyte was being pumped at its maximum rate of 1.7 liters/min. This fact was demonstrated in six different switchings of the magnetic field. (It was shown, however, that when the pumping speed is decreased it is possible to obtain addtional lowering of the cell voltage by application of an external $\vec{B}$ field.)

From the data given in Table IX, it is seen that for those cases with both electrodes or just the cathode between the pole pieces that a sizeable portion of the total voltage drop obtained through the combination of pumping and applied magnetic field was obtainable with just the application of the $\vec{B}$ field.

What the preceding is saying is that there is apparently a certain amount by which the cell voltage can be lowered due to the combination of pumping the electrolyte and subjecting the electrodes to an applied magnetic field. Once this limit is approached, there is very little additional lowering of the cell voltage associated with either

increasing the pumping speed or the strength of the applied magnetic field. From the results obtained with the maximum pumping speed and the maximum applied $\vec{B}$ field, this point was apparently being approached for both the earlier data described in the text and that given in Table IX.

RELATIONSHIP OF EXPERIMENTAL RESULTS TO EXISTING LITERATURE

The papers which are most closely related to our work with copper were presented by Mohanta (5) and Mohanta and Fahidy (3, 4).

The principal differences between the experiments described in the preceding literature and those conducted for this thesis are as follows:

1) Our current density was more than double their highest value.
2) Their concentration of H_2SO_4 was higher (by over a factor of three in most cases.)
3) Our maximum applied $\vec{B}$ field was greater (their maximum being 0.785 tesla).
4) And probably most importantly in their experiments both electrodes were always placed between the pole pieces.

No experimental data is given (3, 4, 5) concerning effects observed on the cell voltage following the application of a $\vec{B}$ field to a single anode.

CHAPTER V

SUMMARY AND CONCLUSIONS

From chapter III, it appears that there are three principal effects associated with the application of magnetic fields to single electrodes during the electrolysis of water. The first of these is that the apparent solubility of O_2 and H_2 increases when the corresponding electrode is exposed to an applied magnetic field. The other two effects are temperature effects, with the first one being explainable in terms of increased thermal conductivity due to stirring associated with the applied $\vec{B}$ field. The second temperature effect appears to be related to an effect discussed in several French papers (7, 9, 10), for which heating was observed in the direction of the Lorentz force.

The results in Chapter IV demonstrated that when the $\vec{B}$ field is applied to either or both electrodes, during the electrodeposition of copper, that a decrease in the cell voltage is observed. Based on the data presented in Table IX, the decrease observed for the single cathode was, on the average, 1.49 times larger than that observed for the combination of both electrodes between the pole pieces and an average of 8.6 times larger than that observed for the single anode. This decrease in cell voltage appears to be explainable in terms of decreasing the apparent thickness of the diffusion layer near the anode and cathode.

Superimposed on the lowering of the cell voltage is the magnetoresistance associated with the applied $\vec{B}$ field. This magnetoresistance offers an explanation for the fact that the voltage drop observed with just the cathode between the pole pieces was greater than that observed for the combination of both electrodes.

REFERENCES

1. Ernest H. Lyons, Jr., Introduction to Electrochemistry, chapter 4, pages 23-26, chapter 5, pages 51-59, D.C. Heath and Company, Boston (1967).

2. D. Laforgue-Kantzer, Electrochim. Acta 10, 585 (1965).

3. S. Mohanta and T.Z. Fahidy, Can. J. Chem. Engng. 50, 248 (1972).

4. S. Mohanta and T.Z. Fahidy, Electrochim. Acta 19, 835 (1974).

5. S. Mohanta, M.S. Thesis, The University of Waterloo, (1971).

6. H.H. Wieder, Hall Generators and Magnetoresistors, chapter 1, pages 1-3, Pion Limited, London (1971).

7. E. Tronel-Peyroz, A. Olivier and D. Laforgue-Kantzer, Electrochim. Acta 22, 145 (1977).

8. E. Tronel-Peyroz, A. Oliver, T.Z. Fahidy and D. Laforgue-Kantzer, Electrochim. Acta 25, 441 (1980).

9. E. Tronel-Peyroz, A. Oliver, C. r. hebd. Se'anc. Acad. Sci. Paris Serie C 278, 997 (1974).

10. J. Pages-Nelson, Annales de Physique 4, 447 (1969).

11. Robert Stow, AIM 65 Microcomputer User's Guide, chapter 1, pages 1-6, Rockwell International Corporation (1978).

12. Carl F. Prutton and Samuel H. Maron, Fundamental Principles of Physical Chemistry, chapter 6, pages 181-184, chapter 7, pages 210-213, The MacMillian Company, New York (1953).

13. Robert C. Weast, Editor, CRC Handbook of Chemistry and Physics, pages D-157, D-159, 55th Edition, CRC Press, Inc (1974).

14. Francis W. Sears and Gerhard L. Salinger, Thermodynamics, Kinetic Theory, and Statistical Thermodynamics, chapter 8, pages 216-218, Addison-Wesley Publishing Company (1975).

15. C.L. Mantell, Electrochemical Engineering, chapter 5, pages 55, 57, 4th edition, McGraw-Hill Book Company, Inc, New York (1960).

APPENDIX

Several minor variations of the same computer program were utilized during the collection and processing of data for the experiments discussed in Chapters III and IV, with the principal variables being that type of data and the order in which the data was taken.

Because all of the programs were basically the same, only the variation utilized for the experiments conducted under the constant current mode is given below:

```
1 REM PROGRAM NAME
CACO1, PLEASE INPUT
X1 AND U IN MINUTES

3 TC=19. 57:INPUT "N"
:N

4 REM N=1 TO SET PH
METER; N=0 TO RUN PR
OGRAM

5 A=0:INPUT"FREQ";X
1=INPUT"INTERVAL";U

6 POKE40961, A

7 C5=.1

8 CD=0:Q=0

10 FOR I=1TO50:READ
X:POKE4045+I,X:NEXTI

20 DATA72,138,72,23
0,223,166,223,224,16
,208,32

30 DATA169,0,133,22
3,230,222,162,60,228
,222,208,20

40 DATA133,222,230,
221,228,221,208,12

50 DATA133,221,230,
220,162,24,228,220,2
08,2

60 DATA133,220,104,
170,173,244,111,104,
64

70 FORI=1TO4:READX:
POKE219+I,X:NEXTI

80 DATA0,0,0,0

90 POKE28670,192:P
OKE28667,64

100 POKE41984,206:P
OKE41985,15
```

```
110 POKE28660,34:PO
KE28661,244

111 GOTO2000

112 H=0:GOTO145

139 A=A

140 POKE 28659,0

142 GOSUB580

145 POKE28659,0

150 POKE28658,123

160 POKE 28668,207

170 POKE 28656,0

180 X=PEEK(28657)

190 POKE 28668,239

200 POKE 28668,207

210 WAIT28669,2

220 X=PEEK(28657)

230 Y=PEEK(28656)

240 POKE 28656,1

250 Y=PEEK(28657)

260 POKE 28656,2

261 B=PEEK(28656)

262 IF B=134THENB=-
1

263 IFB=130THENB=1

270 Z=PEEK(28657)

280 RD1=INT(X/16)

290 R=INT(RD1/2)+1

300 D1=(RD1/2-INT(R
D1/2))*2

310 D2=X-RD1*16

320 D3=ITN(Y/16)

330 D4=Y-3*16

340 D5=INT(Z/16)

350 D6=Z-D5*16

360 F1=D1*100000+D2
*10000+D3*1000+D4*10
0+D5*10+D6

362 F1=B*F1

370 W=INT(X/32)

375 IFA=OTHENPRINT"
":PRINT"SOR  VOLTAG
E TIME(M)"

380 ON W GOTO 430,4
60,490,520,550

430 G1=F1/10000:A$=S
TR$(G1):A$=A$+"M"

435 E=G1/1000

440 GOTO560

460 G2=F1/100000:A$
=STR$(G2):A$=A$+"V"

465 E=G2

470 GOTO560

490 G3=F1/10000:A$=
STR$*(G3):A$=A$+"V"

495 E=G3

500 GOTO560

520 G4=F1/1000:A$=S
TR$(G4):A$=A$+"V"
```

```
525 E=G4

530 GOTO560

550 G5=F1/100:A$=ST
R$(G5):A$=A$+"V"

555 E=G5

558 IFA=0GOTO590

560 ONAGOTO750,750,
4000

565 PRINT"CV ";A$;T
AB(12);H

566 NO=INT((E-8.4)*
4095)

570 GOTO139

580 H=H+.005

585 H=INT((H-A*U)/X
1)

590 H=X1*H+A*U

620 A=A+1

630 IFA=4THENA=0

640 POKE40963,255

650 POKE40961, A

660 H1=H

665 B=H1+X1-3*U-.00
5

666 C=H1=U-.005

668 IFA=0THEN670

669 GOTO710

670 H=PEEK(220):M=P
EEK(221):S=PEEK(222)

680 IFH<BTHEN670

690 IFH<BTHEN670

700 RETURN

710 H=PEEK(220):M=P
EEK(221):S=PEEK(222)

720 H=60*H+M+S/60

730 IFH<CTHEN710

740 RETURN

750 C1=3.975E-5:C2=
1.25E-8:C3=0

760 T=(-C1+SQR(C1*C
1+4*EC2))/(2*C2)

770 T=INT(T*100)/10
0

780 PRINT"TC ";T;TA
B(12);H

785 NO=INT((T-22)*4
09.5)

790 GOTO139

800 IFN=1THEN860

802 PH=(E/C5)

805 GOSUB1000

810 PH=(INT(PH*1E4)
)/1E4

820 PRINT"PH ";PH;T
AB(12);H

825 NO=INT((PH+.3)*
4095)

830 GOTO139

860 PH2=4
```

```
682 C6=2.449E-2:C7

870 PH1=PH2/(1+(T-T
C)*C6+(T-TC)*(T-TC)*
C7)

875 PH1=(INT(PH1*1E
4))/1E4

880 PRINT"PH1";PH1;
TAB(12);H

885 NO=INT((PH-1)*4
09.5)

890 GOTO139

1000 FORI=1TO10

1010 C6=(5.81E-2)*E
XP(-.216*PH):C7=-C6/
21.83

1020 PH=(E/C5)*(1+(
T-TC)*C6+(T-TC)*(T-T
C)*C7)

1030 NEXTI

1040 RETURN

1100 GOTO139

1200 GOTO139

1300 GOTO139

1400 GOTO139

1500 GOTO139

2000 POKE04,0

2010 POKE04,0

2020 POKE05,43

2030 FORL1=1TO27

2040 READXA

2050 POKEDA+L1,XA

2060 NEXTL1

2070 DATA72,8,173,2
49,42,141,252,159,10
6,106

2080 DATA106,106,14
1,253,159,173,250,42
,141,254

2090 DATA159,141,25
5,159,40,104,96

2100 GOTO112

3010 DP=11001

3020 N1=INT(NO/256)

3030 N2=NO-N1*256

3040 POKEDP,N2

3050 POKEDP+1,N1

3060 YA=USR(I)

3070 RETURN

4000 CC=INT((E/.112
5)*1E6)/1E6

4010 PRINT"CC ";CC;
TAB(12);H

4020 Q=INT(CC*H*60*
1E2)/1E2

4030 CD=CC

4040 PRINT"COU PASS
";Q

4050 GOTO130
```

Since the cell current was nearly constant, the cell voltage was considered to be of greater experimental importance. For this reason, the cell voltage was read first, then the two temperature readings (near the anode and cathode), followed in turn by the cell current. If the cell voltage was "constant" instead the only difference would be that the cell current should be read first.

The program listed can be divided in to a number of primary sections as follows:

A. Line 3 tells the computer if the pH meter is merely being set or if the experiment is actually running.

B. Lines 5-6 enters the variables which determine the frequency with which each individual type of data is read along with the interval between two succeeding data points. Also A, which determines the channel to be monitored, is set to 0.

C. Lines 10-110 set and regulate the clock which determines when the data should be taken. This clock is controlled by the computers internal clock.

D. Lines 145-270 transfer the voltage value from the DMM to AIM 65 and defines several important variables in accordance with the data transferred.

E. Lines 280-555 determine the decimal form of the voltage value including its sign and the scale the DMM was on when the reading was taken.

F. Lines 558-560 determine what is to be done with this voltage value based on the value of A (for A = 1, 2 or 3). If A = 0 this taken care of by lines 440, 470, 500 and 550.

G. Line 565 prints the cell voltage.

H. Lines 750-780 determine and print the temperature as measured by the thermocouple.

I. Lines 800-830 and 1000-1040 are used for the determination and printing of the pH, including temperature corrections.

J. Lines 860-885 are used to calibrate the pH meter using a standard buffer solution.

K. Lines 4000-4010 are used to calculate and print the cell current.

L. In conjunction with the calculation of the cell current, when the constant current mode is utilized the number of coulombs passed is determined and recorded by lines 4020-4040.

M. Lines 580-666 define some variables required to keep the readings synchronized with the clock portion of the program and incorporate a few small constants to take care of round off errors. The value of A is also reset in this section of the program.

N. Lines 670-690 maintain the correct frequency over the course of the run.

O. And in a similar manner lines 710-730 maintain the correct interval.

P. Lines 2000-3070 were included to control a digital to analog converter which was added to allow for the direct graphing of data by the AIM 65. Due to hardware problems this portion of the program was not used during any of the runs.

It should be noted that some of the above sections were by passed when deemed appropriate based on the nature of the experiment. For instance during most of the experiments discussed in Chapter III the only data monitored was cell voltage and cell current along with various temperatures.